Synthesis and Characterization of Halogeno- and Pseudohalogeno-thallium(III) Porphyrin Complexes. Variation of the Co-ordination Geometry as a Function of the Axial Ligand†

Mathias O. Senge,* Karin Ruhlandt-Senge, Kevin J. Regli and Kevin M. Smith
Department of Chemistry, University of California, Davis, CA 95616, USA

Several thallium(III) porphyrin complexes [Tl(por)X] with the axial ligand X = $MeCO_2$, CF_3CO_2, Cl, Br, I, CN, SCN or N_3, have been obtained *via* ligand-exchange reactions from the corresponding thallium(III) trifluoroacetates. All compounds were characterized by ^1H NMR, UV/VIS spectroscopy, and elemental analysis. Fourteen compounds were investigated in detail by X-ray crystallography to obtain information on the influence of the axial ligand on the macrocycle core conformation in main-group metalloporphyrins and to establish the molecular stereochemistry of thallium(III) porphyrins with cyano, acetato, thiocyanato, bromo, iodo and azido groups as axial ligands.

The study of the co-ordination geometry in metalloporphyrins has wide implications for the structural chemistry, catalytic activity and *in vivo* function of tetrapyrrole metal complexes.[1] We are interested in the influence of the axial ligand on the core and macrocycle properties with regard to the role of co-ordinating protein functionalities in pigment–protein complexes *in vivo*.[2] It has been proposed that different macrocyclic conformations of porphyrins induced by interaction with the protein are responsible for the different physicochemical properties observed in porphyrin–protein complexes.[3] Porphyrin complexes of the main Group III elements Al,[4] Ga,[5–7] In,[8–11] and Tl[12–18] are very suitable model compounds since they show considerable flexibility of the core geometries depending on the axial ligands at the metal centre.[1] In order to obtain a metalloporphyrin series with different axial ligands suitable for structural and physicochemical studies we decided to synthesise the complete halogenothallium(III) series of the porphyrins illustrated and also investigate the stereochemistry of the related pseudohalogeno complexes. During preparation of this work for publication we became aware of related work recently published by Coutsolelos and co-workers, who described the preparation and crystal structure of [Tl(tpp)F][19] and [Tl(tpp)(NC)][20] as well as the synthesis of some of the (pseudohalogeno)thallium porphyrins described here.

Results and Discussion

Syntheses.—The reaction of free-base porphyrins with thallium(III) acetate or trifluoroacetate affords the corresponding six-co-ordinate thallium(III) porphyrins in high yield.[13,21–23] As worked out earlier by Smith and co-workers,[21] these compounds present versatile reagents for the preparation of related thallium(III) porphyrin complexes *via* ligand-exchange reactions. Simple stirring of [$TlL(O_2CCF_3)$] (L = porphyrinate) with KX in CH_2Cl_2–MeOH or tetrahydrofuran afforded a variety of halogeno- and pseudohalogeno-thallium(III) porphyrin complexes. The yields of the halogeno complexes (X = Cl, Br or I) were generally higher (85–95%) than those of the pseudohalogeno complexes [X = CN (88–92), N_3 (80–90) or SCN (76–80%)]. The preparation of some of the pseudohalogeno complexes described here and of two thallium(III) fluoroporphyrins were recently described by Coutsolelos *et al.*[19,20] These workers used a slightly different synthetic route involving water and the use of 18-crown-6 (1,4,7,10,13,16-hexaoxacyclooctadecane); the yields are however comparable. Purification of the porphyrins *via* column chromatography was not necessary and was avoided to prevent ligand exchange with chloride or water from the column material.[13]

Spectroscopy.—The NMR data for the porphyrins studied are given in the Experimental section. No significant axial-ligand-dependent differences in the chemical shifts of the β-pyrrole hydrogens or the phenyl signals are observed. Similar results were observed for a related gallium(III) porphyrin series[24] and this can be attributed to the heavy central metal for which deshielding properties are more important than is the influence of the axial ligand.[19] Coupling between ^1H and $^{203,205}Tl$[25] is observed for the β-pyrrole hydrogens but not for the phenyl signals.[22] An interesting difference in the ^1H–Tl couplings between the *meso*-hydrogen splitting and the β-hydrogen splitting can be observed. While in the oep series[22] the coupling constants of the *meso*-hydrogen get smaller with increasing electron withdrawal, in the present halogeno series the coupling constant for the β-hydrogen signals increases in the series I < Br < Cl ≈ F (J = 52 for I, 60 for Br, 63 for Cl, 64 Hz for F[19]). The ^{13}C NMR spectroscopy of thallium porphyrins has been investigated in detail by Abraham *et al.*[26]

The electronic absorption spectra (see Experimental section) show the two-banded spectra typical of many metalloporphyrins, as already noted in many publications on thallium(III) porphyrins.[22] The complete halogeno series presented here allows however some conclusions with regard to the influence of different axial ligands on the properties and stability of the central metal atom. No drastic influence of different axial ligands on the wavelength of the main absorption bands is observed although there is a trend towards higher wavelengths with increasing size of the halogen atom. The intensity ratio of the β and α bands can be used as a rough estimate of the stability of the central metal, those with numerically larger ratios being considered more stable.[27] The data for the [Tl(tpp)X] series are listed in Table 1. With the exception of the chloride complex there seems to be a trend to higher stability in the halogeno series. Similar data were found in the tmpp series and oep series.[20,28] In the tpp series the thiocyanato complex has the

---

† *Supplementary data available:* see Instructions for Authors, *J. Chem. Soc., Dalton Trans.*, 1993, Issue 1, pp. xxiii–xxviii.

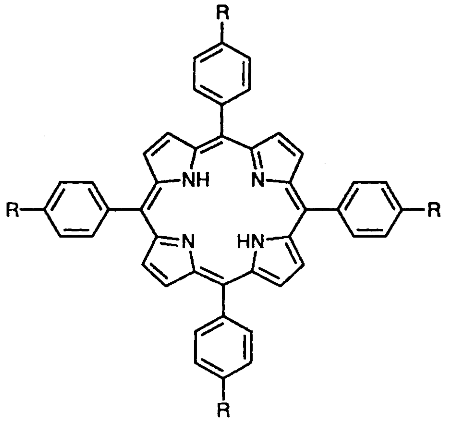

H_2tpp R = H
H_2tmpp R = OMe

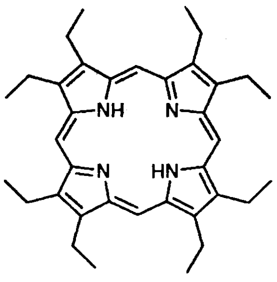

H_2oep

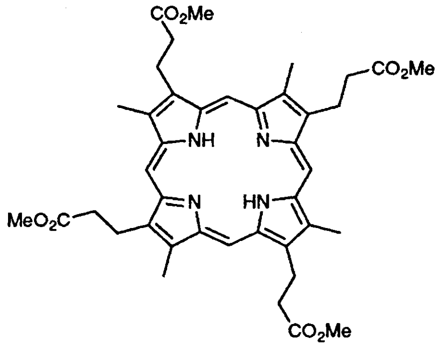

H_2L^1

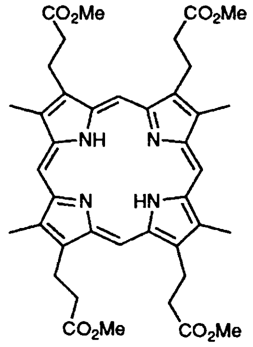

H_2L^2

Table 1 Wavelengths and absorption ratios of the α and β bands in the absorption spectra of the [Tl(tpp)X] porphyrins studied in CH_2Cl_2

	λ/nm		
X	α band	β band	Absorption ratio (β/α)
CF_3CO_2	566	606	0.67
F	569	609	0.50[a]
Cl	566	608	0.63[b]
Br	566	606	0.57
I	570	610	0.62
CN	568	608	0.64
SCN	568	608	0.87
N_3	564	606	0.56

[a] From ref. 19, in $CHCl_3$. [b] Ref. 28.

highest α : β ratio of 0.87 : 1, while in the tmpp series this value is 1.10 : 1 for the SCN complex and 1.16 : 1 for the cyanato complex. In general higher ratios were found for the tmpp compared to the tpp or oep derivatives.

Initial mass spectrometric investigations gave results similar to those already noted in the literature, *i.e.* base peaks observed correspond mainly to the metal-free ligand system and therefore are not useful for characterization of the intact porphyrin–axial ligand system, only for the macrocyclic system.[29]

Structural Descriptions.—The main thrust of this contribution is the structural characterization of the stereochemistry at the central thallium atom of the porphyrin complexes and the investigation of the different metal–axial ligand combinations on the macrocycle conformation. We have therefore made extensive use of X-ray crystallography to characterize most of the synthesised complexes structurally. The main crystal data and refinement details are compiled in Table 2 while the atomic co-ordinates of the porphyrins studied are listed in Tables 6–18. With the exception of the acetatothallium complexes all structures exhibit a typical five-co-ordinated thallium(III) centre co-ordinated to the four pyrrole nitrogen atoms of the macrocyclic system and to the axial ligand.

Acetato complexes. Fig. 1 shows the molecular structure of $[TlL^2(O_2CMe)]$. Overall, this structure and that of $[TlL^1(O_2CMe)]$ (not shown) exhibit very similar characteristics. The main difference is that the latter complex crystallizes with one molecule of solvation (CH_2Cl_2) per porphyrin macrocycle. The thallium atoms are six-co-ordinated to the four pyrrole nitrogens and to the two oxygen atoms of the acetato ligand. The axial ligand binds in a symmetric bidentate fashion to the thallium atom with average bond lengths of 2.394(7) Å in $[TlL^1(O_2CMe)]$ and 2.388(7) Å in $[TlL^2(O_2CMe)]$ (Table 3). These bond lengths are slightly longer than those observed in thallium(III) acetate, where Tl–O bond lengths of 2.26–2.31(1) Å were observed.[30a] An asymmetric bidentate thallium acetate complex showed Tl–O bond distances of 2.38 and 2.53 Å.[30b] An even larger spread of Tl–O distances was found in the crystal structure of thallium(III) acetate monohydrate, ranging from 2.17 to 2.78(1) Å.[30c] Thallium(III) dimethylacetate showed Tl–O distances ranging from 2.4 Å to 2.61(2) Å.[30d] Hydroxobis(pentafluorophenyl)thallium(III) with a single co-ordinated oxygen, exhibited a Tl–O bond length of 2.23(2) Å, which is closest to the value expected on the basis of Pauling's covalent radii.[30e] Other Tl^{III}–O distances found in the literature are considerably longer and range from 2.4 to 2.9 Å.[31] The O–Tl–O

Table 2 Summary of crystal data, data collection and refinement for the thallium porphyrins studied[a]

	[TlL^1(O$_2$CMe)]	[TlL^2(O$_2$CMe)]	[Tl(tmpp)Cl]	[TlL^1(Cl)]	[Tl(tpp)I]	[Tl(tmpp)I]	[Tl(tpp)(CN)]
Formula	$C_{42}H_{47}N_4O_{10}Tl\cdot CH_2Cl_2$	$C_{42}H_{47}N_4O_{10}Tl$	$C_{48}H_{36}ClN_4O_4Tl$	$C_{40}H_{44}ClN_4O_8Tl\cdot CH_2Cl_2$	$C_{44}H_{28}IN_4Tl$	$C_{48}H_{36}IN_4O_4Tl\cdot CH_3OH$	$C_{45}H_{28}N_5Tl$
M	1054.1	972.2	972.6	1031.5	944	1096.1	843.1
Colour	Red	Red	Purple	Purple	Purple	Purple	Purple
Crystal size/mm	0.44 × 0.19 × 0.13	0.6 × 0.3 × 0.22	0.7 × 0.35 × 0.28	0.86 × 0.08 × 0.04	0.6 × 0.36 × 0.24	0.78 × 0.35 × 0.18	0.65 × 0.32 × 0.21
Crystal system	Triclinic	Monoclinic	Triclinic	Triclinic	Monoclinic	Triclinic	Monoclinic
Space group	$P\bar{1}$	$P2/c$	$P\bar{1}$	$P\bar{1}$	$P2_1/n$	$P\bar{1}$	$P2_1/n$
a/Å	13.201(6)	13.385(7)	11.661(6)	12.304(12)	9.823(3)	11.690(4)	9.932(4)
b/Å	13.882(6)	24.730(16)	11.802(5)	12.971(8)	16.514(5)	12.410(3)	16.042(5)
c/Å	14.250(7)	12.434(4)	14.654(5)	14.049(11)	21.605(8)	15.680(4)	21.209(9)
α/°	80.43(4)	90	97.43(3)	79.84(4)	90	85.39(2)	90
β/°	65.81(3)	104.79(2)	95.10(3)	67.23(3)	90.75(3)	69.16(2)	90.92(3)
γ/°	64.96(4)	90	94.21(4)	82.00(4)	90	79.57(2)	90
U/Å^3	2158(2)	3979(4)	1984.5(15)	2029(3)	3504(2)	2090.3(10)	3379(2)
Z	2	4	2	2	4	2	4
D_c/Mg m^{-3}	1.573	1.624	1.628	1.627	1.791	1.735	1.657
μ/mm^{-1}	3.958	4.160	4.227	9.977	5.564	4.684	4.868
F(000)	1022	1056	964	1028	1816	1072	1656
Diffractometer	Siemens R3m/V	Siemens R3m/V	Syntex P2$_1$	Siemens P4/RA	Siemens R3m/V	Siemens R3m/V	Siemens R3m/V
Scan speed/° min^{-1}	29.30	58.59	29.30	58.59	29.30	29.30	29.30
Scan range/°	2.00	1.60	2.2	1.60 + Kα separation	1.60	1.60	2.00
Octants collected	$\pm h, \pm k, +l$	$\pm h, +k, +l$	$\pm h, \pm k, +l$	$\pm h, \pm k, +l$	$\pm h +k, +l$	$\pm h, \pm k, +l$	$+h, +k, \pm l$
g	0.0001	0.0011	0.0024	0.0017	0.0030	0.0033	0.0090
Independent reflections	9929	6572	9716	4969	8049	9596	7761
Observed reflections	7199	6039	6714	4463	5739	6964	5406
	$[F > 5.0\sigma(F)]$	$[F > 6.0\sigma(F)]$	$[F > 6.0\sigma(F)]$	$[F > 3.0\sigma(F)]$	$[F > 6.0\sigma(F)]$	$[F > 6.0\sigma(F)]$	$[F > 4.5\sigma(F)]$
No. of parameters	546	514	522	519	326	546	465
Δ/σ	0.096	0.026	0.003	0.118	0.177	0.048	0.088
ρ_{max}/e Å^{-3}	1.26 (near Tl)	1.88 (near Tl)	1.78 (near Tl)	2.76 (near Tl)	2.95 (near Tl)	2.40 (near Tl)	2.14 (near Tl)
R^b	0.037	0.041	0.042	0.067	0.055	0.057	0.057
R'^c	0.039	0.051	0.055	0.085	0.070	0.087	0.073
S	1.36	1.08	0.88	1.65	1.03	1.24	1.02

Table 2 (*continued*)

	[Tl(tmpp)(CN)]	[Tl(oep)(CN)]	[Tl(tpp)(SCN)]	[Tl(tmpp)(SCN)]	[Tl(tpp)(N_3)]	[Tl(tmpp)(N_3)]	[Tl(tpp)Br]
Formula	$C_{49}H_{36}N_5O_4Tl$	$C_{37}H_{44}N_5Tl$	$C_{45}H_{28}N_5STl$	$C_{49}H_{36}N_5O_4STl\cdot 2CH_2Cl_2$	$C_{44}H_{28}N_7Tl$	$C_{48}H_{36}N_7O_4Tl\cdot CH_2Cl_2$	$C_{44}H_{28}BrN_4Tl$
M	963.2	763.1	875.2	1165.1	859.1	1064.1	897.0
Colour	Purple	Purple	Purple	Purple	Purple	Purple	Purple
Crystal size/mm	0.65 × 0.27 × 0.18	0.85 × 0.38 × 0.22	0.85 × 0.22 × 0.1	0.8 × 0.37 × 0.29	0.43 × 0.18 × 0.1	0.7 × 0.39 × 0.21	0.24 × 0.22 × 0.22
Crystal system	Triclinic	Triclinic	Triclinic	Triclinic	Triclinic	Triclinic	Monoclinic
Space group	$P\bar{1}$	$P\bar{1}$	$P\bar{1}$	$P\bar{1}$	$P\bar{1}$	$P\bar{1}$	$P2_1/n$
a/Å	11.616(4)	10.537(2)	10.970(3)	11.834(2)	10.801(4)	11.152(3)	9.860(4)
b/Å	11.994(2)	10.663(2)	12.620(3)	14.660(3)	12.714(6)	14.313(4)	16.244(6)
c/Å	14.553(5)	15.605(3)	14.533(3)	15.521(5)	14.247(3)	15.439(5)	21.381(10)
α/°	96.53(2)	109.36(1)	80.73(2)	117.54(2)	81.19(3)	68.65(2)	90
β/°	96.81(2)	102.34(2)	70.35(2)	97.03(2)	70.59(3)	87.72(2)	90.13(4)
γ/°	94.74(2)	97.82(1)	67.63(2)	97.20(2)	67.28(3)	70.45(2)	90
U/Å^3	1999.7(9)	1574.6(5)	1750.9(7)	2318.5(10)	1701.4(11)	2153.6(11)	3424(3)
Z	2	2	2	2	2	2	4
D_c/Mg m^{-3}	1.607	1.610	1.660	1.670	1.677	1.638	1.740
$F(000)$	956	764	860	1156	844	1056	1744
μ/mm^{-1}	4.148	5.213	4.756	3.845	4.837	3.965	5.922
Diffractometer	Siemens R3m/V	Siemens R3m/V	Syntex $P2_1$	Siemens R3m/V	Siemens R3m/V	Syntex $P2_1$	Siemens R3m/V
Scan speed/° min^{-1}	29.30	58.59	29.30	58.59	29.30	58.59	8.08
Scan range/°	1.60	1.20	2.00	2.10	1.40	1.20	2.00
Octants collected	$\pm h, \pm k, +l$	$\pm h, \pm k, +l$	$\pm h, \pm k, +l$	$\pm h, \pm k, +l$	$\pm h, \pm k, +l$	$\pm h, \pm k, +l$	$\pm h, +k, +l$
g	0.0007	0.0051	0.0010	0.0007	0.0020	0.0017	0
Independent reflections	9199	7647	8089	10 646	7862	9911	7852
Observed reflections	7070 [$F > 6.0\sigma(F)$]	6009 [$F > 6.0\sigma(F)$]	6340 [$F > 6.0\sigma(F)$]	8400 [$F > 6.0\sigma(F)$]	5520 [$F > 7.0\sigma(F)$]	7649 [$F > 3.5\sigma(F)$]	5245 [$F > 4.0\sigma(F)$]
No. of parameters	532	392	472	599	472	574	451
Δ/σ	0.003	0.067	0.071	0.064	0.115	0.001	0.037
ρ_{max}/e Å^{-3}	1.47 (near Tl)	3.37 (near Tl)	1.97 (near Tl)	1.60 (near Tl)	1.17 (near Tl)	1.70 (near Tl)	0.92 (near Tl)
R^b	0.041	0.050	0.041	0.037	0.045	0.041	0.045
R'^c	0.046	0.067	0.049	0.044	0.056	0.053	0.034
S	0.98	0.86	1.04	1.06	0.92	0.94	1.09

[a] $T = 130$ K, ω scan and $2\theta_{max} = 55°$ except for [TlL^1(Cl)] where $T = 120$ K, 2θ–θ scan and $2\theta_{max} = 108.5°$. [b] $R = \Sigma\|F_o| - |F_c\|/\Sigma|F_o|$. [c] $R' = [\Sigma w(|F_o| - |F_c|)^2/\Sigma wF_o^2]^{\frac{1}{2}}$ where $w^{-1} = \sigma^2(F) + gF^2$.

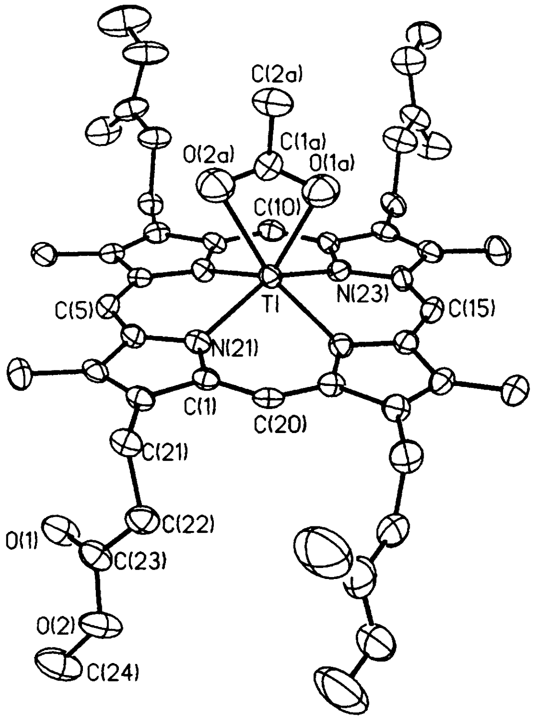

Fig. 1 Computer-generated plot and numbering scheme of $[TlL^2(O_2CMe)]$. Hydrogen atoms have been omitted for clarity; ellipsoids at 50% level

angles of 52.1 and 53.4° found in the L^1 and L^2 complexes are also slightly smaller than those found (*ca.* 55°) in thallium(III) acetate. The C–O bond lengths in the ligand are 1.21 in the L^2 complex and 1.23 Å in the L^1 complex, while the O–C–O bond angles are 117.3(5) and 123.4(5)°, respectively. The O–C–O plane of the axial ligand is not perfectly orthogonal to that of the four nitrogen atoms (4N plane) but deviates by about 9°. The O–C–O vector of the axial ligand is rotated against the axes of opposite nitrogen pairs. These dihedral angles (denoted as φ by Hoard and co-workers[32]) are 27.5° in $[TlL^1(O_2CMe)]$ and 43.4° in $[TlL^2(O_2CMe)]$. Thus the latter value comes nearest to a staggered conformation while the former lies in the middle between the eclipsed and staggered conformation.

Similar results were recently noted by Suen *et al.*[18a] for $[Tl(tpp)(O_2CMe)]$ at room temperature; they found, in solution, bidentate binding of the acetato ligand at low temperature and a symmetric pseudo-chelating binding at room temperature. It was concluded that the solid-state configuration of the axial ligands mimics the form found at low temperature in solution.[18b] Monodentate binding was observed in the structure of an acetatoiron(III) porphyrin with a five-co-ordinated metal centre ligated to only one of the carboxyl oxygen atoms.[33a] The related structure of $[In(oep)(O_2CMe)]\cdot 2CHCl_3$ showed an intermediate situation between end-on and bidentate co-ordination,[33b] while bidentate co-ordination was also found in $[Nb(tpp)O(O_2CMe)]$[33c] and $[Zr(oep)(O_2CMe)_2]$.[33d]

Halogeno complexes. The crystal structures of two chlorothallium(III) porphyrin complexes, [Tl(tmpp)Cl] and $[TlL^1(Cl)]$ were determined; Fig. 2 shows that of the former. The coproporphyrinate I (L^1) complex crystallizes as the methylene chloride solvate. Both compounds exhibit the typical five-co-ordinate thallium centre observed in the two other known TlCl porphyrin structures, [Tl(oep)Cl][12] and [Tl(tpp)Cl].[13] The thallium–chloride bond distances (Table 3) of 2.451(2) and 2.487(4) Å agree well with those observed in the other chlorothallium porphyrins and are also close to those observed in (1,10-phenanthroline)thallium(III) trichloride.[34] They are slightly longer than those observed [2.391(6) Å] in thallium(III) chloride tetrahydrate.[35b] Similarly, shorter Tl–Cl bond lengths were found in trichlorobis(pyridine-4-carbonitrile-1-oxide-*O*)-thallium (2.364 for equatorial Cl and 2.42 Å for axial Cl),[36a] while in a substituted amidine complex of Tl^{III}, $[PhC(NHSiMe_3)_2][TlCl_3\{PhC(NSiMe_3)_2\}]$,[36b] lengths of 2.56 and 2.46 Å were observed. Bond lengths of 2.48 Å were found in the anion of $[Co(NH_3)_6][TlCl_6]$,[36c] while the $[TlCl_4]^-$ anion exhibits distances of 2.392(3) and 2.420(9) Å in $[(Tl^IL)_4CuCl_4][Tl^{III}Cl_4]_2$,[36d] (L = 18-crown-6) similar to those found in $K[TlCl_4]$ and $Tl[TlCl_4]$.[36e] Bridging chloride–thallium bonds are generally longer.[37] The Tl–Cl bond characteristics agree also well with those found in two related macrocyclic systems, *i.e.* [TlL(Cl)] (L = 5,15-dioxo[17] or 5,10,15,20-tetranitro[38] derivative of oep). The Tl–N (porphyrin) bond lengths are similar in both complexes, 2.206(5) Å in [Tl(tmpp)Cl] and 2.204(9) Å in $[TlL^1(Cl)]$. The Cl–Tl–N bond angles are 109.0(2) and 107.5(3)°, respectively.

The complex [Tl(tpp)Br] is the first example of a bromothallium(III) porphyrin and its structure is shown in Fig. 3. The structure is an isotype of the chloride derivative and exhibits the typical five-co-ordinated thallium with a Tl–Br bond length of 2.542(2) Å. This is longer than those observed in $TlBr_3\cdot 4H_2O$ [2.515(3) Å][35b] or tribromobis(dioxane)thallium [2.504(3) Å],[35c] similar to the situation found for Tl–Cl. Smaller Tl–Br bond lengths were also observed in the structure of (pyridine *N*-oxide)thallium(III) bromide[39a] [2.517(1) Å] and tribromobis(triphenylphosphine oxide)thallium(III) [2.504(3) Å],[39b] while the $[TlBr_4]^-$ anion in $[(TlL)_4CuBr_4][TlBr_4]$[39c] (L = 18-crown-6) showed Tl–Br bond lengths of 2.545(2) Å which are quite similar to those observed in the present porphyrin complex. The mixed-halogeno complex bromodiiodobis(4-methylpyridine *N*-oxide)thallium[39d] showed a longer bond distance [2.676(1) Å]. Bond lengths of 2.58 Å were found in $[Co(NH_3)_6][TlBr_6]$,[36c] while in tribomobis(pyridine)thallium (III)[39e] an average bond length of 2.531(9) Å was observed. The Tl–Br–N angles are 109.9(2)° and the average Tl–N (porphyrin) bond length is 2.231(6) Å. The only other metalloporphyrin with bromide as axial ligand known to us is that of $[Ti^{IV}(tpp)Br_2]$ which exhibits Ti–Br bond lengths of 2.454(2) Å.[40]

The complexes [Tl(tpp)I] and [Tl(tmpp)I] are the first examples of structurally characterized iodothallium(III) porphyrins. As an example, Fig. 4 shows the molecular structure of [Tl(tmpp)I]. It crystallizes as a methanol solvate with one molecule of solvation in the asymmetric unit. Both complexes are characterized by fairly long Tl–I bond distances: 2.714(4) Å in [Tl(tpp)I] and 2.727(1) Å in [Tl(tmpp)I]. Very similar bond lengths were found in triiodobis(3-methylpyridine *N*-oxide)thallium[41] [2.703(1) Å] and bromodiiodobis(4-methylpyridine *N*-oxide)thallium[39d] [2.710(1) Å]. These values are in agreement with those expected for covalent single bonds. The I–Tl–N bond angles in the two complexes studied are 111.3(2) and 110.8(6)°, respectively. A direct comparison with the situation in thallium(III) triiodide is not possible since the iodide induces a disproportionation reaction; the structure of Tl^II_3 is known.[42]

Pseudohalogeno complexes. A recent paper on the synthesis and structure of [Tl(tpp)(NC)][20] discussed in detail the binding of cyanide to thallium(III) porphyrins. On the basis of crystallographic and IR spectroscopic evidence it was concluded that CN binds to the thallium as isocyanide. Unaware of the results of Coutsolelos *et al.*[20] we had also determined the crystal structure of this cyanide adduct (Table 1). All relevant data for this structure, determined at low temperature, are listed in the Supplementary Material only. There are no appreciable differences between the two structure determinations. In addition, we present here the crystal structures of the products of reaction of $[Tl(tmpp)(O_2CCF_3)]$ and $[Tl(oep)(O_2CCF_3)]$ with KCN: [Tl(tmpp)(CN)] is shown in Fig. 5 and [Tl(oep)(CN)] in Fig. 6. All three structures show the typical five-co-ordinated thallium with the cyanide ligand bound in a linear fashion.

Table 3 Averaged bond lengths (Å) and angles (°) for the macrocycle atoms of the thallium porphyrins studied *

	[TlL^1(O$_2$CMe)]	[TlL^2(O$_2$CMe)]	[Tl(tmpp)Cl]	[TlL^1(Cl)]	[Tl(tpp)Br]	[Tl(tpp)I]	[Tl(tmpp)I]
M–L	2.394(7)	2.388(7)	2.451(2)	2.487(4)	2.542(2)	2.714(4)	2.727(1)
M–N(porphyrin)	2.219(3)	2.217(6)	2.206(5)	2.204(9)	2.231(6)	2.237(5)	2.220(5)
N–C$_a$	1.376(5)	1.371(8)	1.381(8)	1.361(13)	1.371(9)	1.376(8)	1.384(9)
C$_a$–C$_b$	1.449(7)	1.456(9)	1.436(8)	1.448(16)	1.444(10)	1.440(12)	1.441(13)
C$_a$–C$_m$	1.397(8)	1.394(10)	1.407(8)	1.400(15)	1.424(10)	1.407(11)	1.408(12)
C$_b$–C$_b$	1.364(8)	1.367(10)	1.354(8)	1.358(17)	1.360(10)	1.345(13)	1.374(14)
N–M–N opp.	141.2(2)	141.6(2)	142.0(2)	145.1(4)	140.2(2)	137.4(2)	138.5(3)
N–M–N adj.	83.7(1)	83.8(2)	84.0(2)	84.8(3)	83.4(2)	82.4(2)	82.8(2)
M–N–C$_a$	124.9(3)	124.1(4)	124.5(4)	124.6(7)	124.5(5)	124.4(4)	124.2(5)
N–C$_a$–C$_m$	124.7(5)	124.9(6)	125.9(6)	124.9(10)	126.5(6)	125.5(7)	125.1(7)
N–C$_a$–C$_b$	108.5(5)	108.5(7)	108.0(6)	108.4(9)	108.3(6)	108.4(6)	108.5(7)
C$_a$–N–C$_a$	108.3(4)	108.7(6)	108.1(5)	108.8(9)	108.5(6)	107.8(5)	107.2(5)
C$_a$–C$_m$–C$_a$	128.3(5)	128.9(6)	126.3(6)	129.0(11)	125.9(6)	127.0(8)	126.9(8)
C$_a$–C$_b$–C$_b$	107.3(5)	107.2(6)	107.9(6)	107.2(10)	107.5(6)	107.7(8)	107.8(8)
C$_m$–C$_a$–C$_b$	126.7(4)	126.6(6)	126.0(6)	126.6(10)	125.2(6)	126.0(7)	126.3(8)

	[Tl(tmpp)(CN)]	[Tl(oep)(CN)]	[Tl(tpp)(SCN)]	[Tl(tmpp)(SCN)]	[Tl(tpp)(N$_3$)]	[Tl(tmpp)(N$_3$)]
M–L	2.193(7)	2.215(8)	2.527(2)	2.552(2)	2.202(9)	2.205(6)
M–N(porphyrin)	2.218(5)	2.220(4)	2.208(3)	2.210(3)	2.218(4)	2.204(4)
N–C$_a$	1.376(8)	1.378(7)	1.377(6)	1.376(5)	1.372(6)	1.380(6)
C$_a$–C$_b$	1.436(8)	1.454(9)	1.439(8)	1.438(7)	1.447(9)	1.437(8)
C$_a$–C$_m$	1.408(8)	1.399(8)	1.409(7)	1.411(7)	1.406(9)	1.411(8)
C$_b$–C$_b$	1.357(8)	1.375(9)	1.351(9)	1.350(8)	1.356(10)	1.354(8)
N–M–N opp.	140.2(2)	139.8(2)	141.7(2)	141.6(1)	141.5(2)	142.5(2)
N–M–N adj.	83.4(2)	83.2(2)	83.8(1)	83.8(1)	83.8(1)	84.8(1)
M–N–C$_a$	124.5(4)	123.8(4)	124.5(3)	124.3(3)	124.1(4)	124.4(3)
N–C$_a$–C$_m$	126.0(5)	124.7(6)	125.7(4)	126.0(4)	126.4(5)	125.7(5)
N–C$_a$–C$_b$	108.3(5)	109.0(5)	108.4(4)	108.1(4)	107.9(5)	108.2(5)
C$_a$–N–C$_a$	108.1(5)	108.0(5)	107.9(3)	108.1(4)	108.9(4)	108.0(4)
C$_a$–C$_m$–C$_a$	126.0(5)	128.5(6)	126.6(5)	125.9(5)	126.2(6)	126.5(5)
C$_a$–C$_b$–C$_b$	107.7(5)	107.1(5)	107.7(5)	107.8(5)	107.6(6)	107.8(5)
C$_m$–C$_a$–C$_b$	125.7(5)	125.7(6)	125.9(4)	125.9(4)	125.6(6)	126.2(5)

* C$_m$ = C(5), C(10), C(15), C(20); C$_a$ = C(1), C(4), C(6), C(9), C(11), C(14), C(16), C(19); C$_b$ = C(2), C(3), C(7), C(8), C(12), C(13), C(17), C(18).

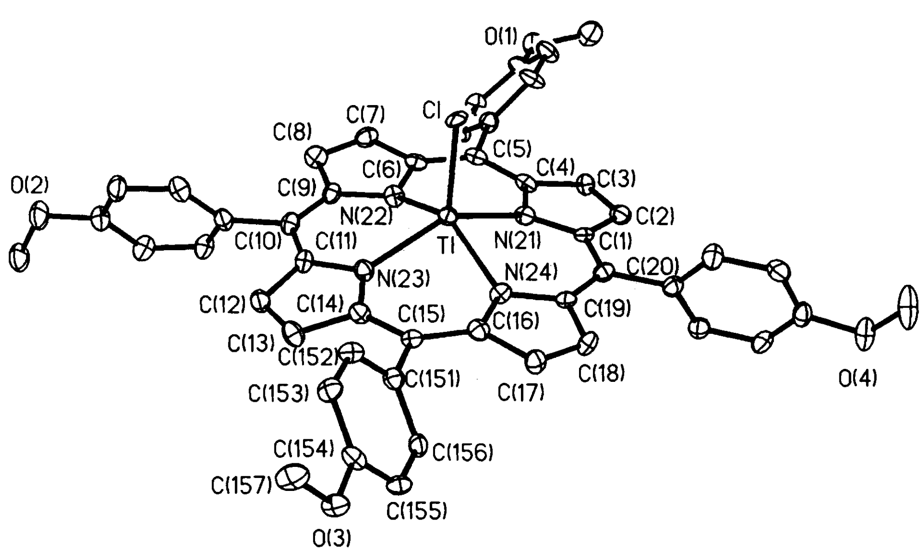

Fig. 2 Computer-generated plot and numbering scheme of [Tl(tmpp)Cl]

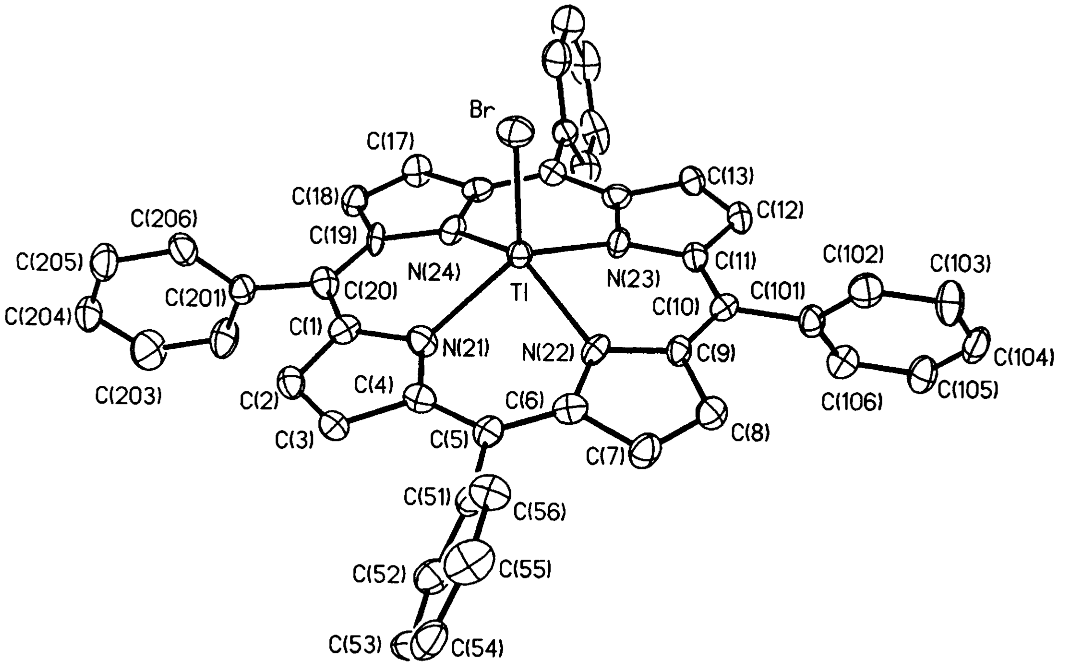

Fig. 3 Computer-generated plot and numbering scheme of [Tl(tpp)Br]

We were not able unambiguously to solve the dichotomy of isocyanide *versus* cyanide binding to the thallium centre on the basis of the crystallographic data. The structures of the Tl(tpp), Tl(tmpp) and Tl(oep) complexes gave no significant differences in the final *R* values or *S* between refinement of the ligand bonded *via* N (isocyanide bonding) or C (cyanide bonding). An inspection of the thermal parameters obtained for the C and N atoms in both refinement strategies pointed however more in the direction of cyanide bonding. In all three cases refinement of the ligand as isocyanide gave considerably smaller thermal parameters for the outer atom than refinement as cyanide. Since the outer atom of the ligand should show higher thermal motion this indicates a preference for the cyanide binding type. Thus, on the basis of our data for three different thallium(III) porphyrins, we are slightly in favour of these complexes being of the cyanide type. The data and figures given for these complexes are those of the refinement as cyanide, without ruling out the possibility of *e.g.* a disordered system with both CN and NC present. The thallium–ligand bond lengths were 2.193(7) Å in [Tl(tmpp)(CN)] and 2.215(8) Å in [Tl(oep)(CN)] and are thus only marginally smaller than those of Coutsolelos *et al.*[20] for (Tl(tpp)(NC)] at room temperature [2.260(3) Å]. In our low-temperature study of [Tl(tpp)(CN)] we found 2.229(6) Å. For comparison, the Tl–C bond length in [Tl(tpp)Me][13] was found to be 2.147(12) Å. The Tl–C bond lengths in small organometallic molecules are normally in the range 2.05–2.16 Å.[30b,d,31b,c37,43a–c] while in TlMe$_3$[43d] longer bonds of up to 2.34(9) Å are observed. The bond lengths within the axial ligand are on average 1.111 Å in the three complexes studied and are comparable to those found in other cyanometal porphyrins.[44] The Tl–C–N or Tl–N–C group is essentially linear with bond angles of 176.6(8), 177.6(8) and 175.9(8)° in the tpp, oep and tmpp derivatives, respectively.

A much clearer situation is found in the characterization of the reaction products of Tl(O$_2$CCF$_3$) porphyrins with KSCN. Fig. 7 shows as an example the molecular structure of [Tl(tpp)(SCN)]. The corresponding tmpp derivative crystallized with two molecules of solvation (methylene chloride) in the asymmetric unit. The structures are characterized by a bent arrangement of the axial ligand with respect to the macrocycle plane. The Tl–S–C angles are 96.5(3)° in [Tl(tpp)(SCN)] and 95.2(2)° in [Tl(tmpp)(SCN)]. The SCN vector is tilted by 86 and

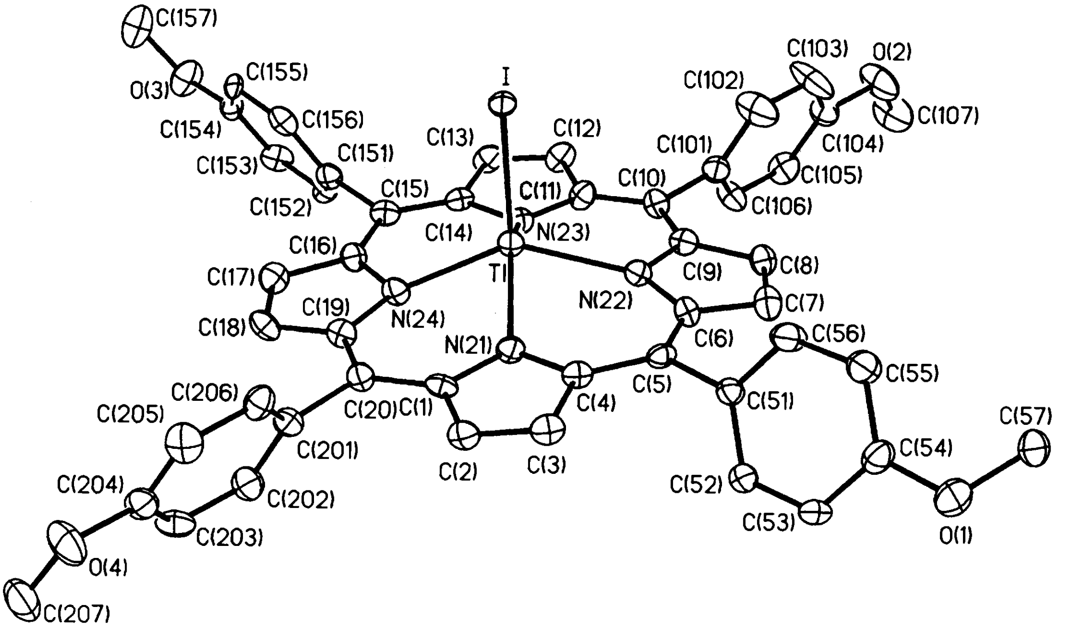

Fig. 4 Computer-generated plot and numbering scheme of [Tl(tmpp)I]

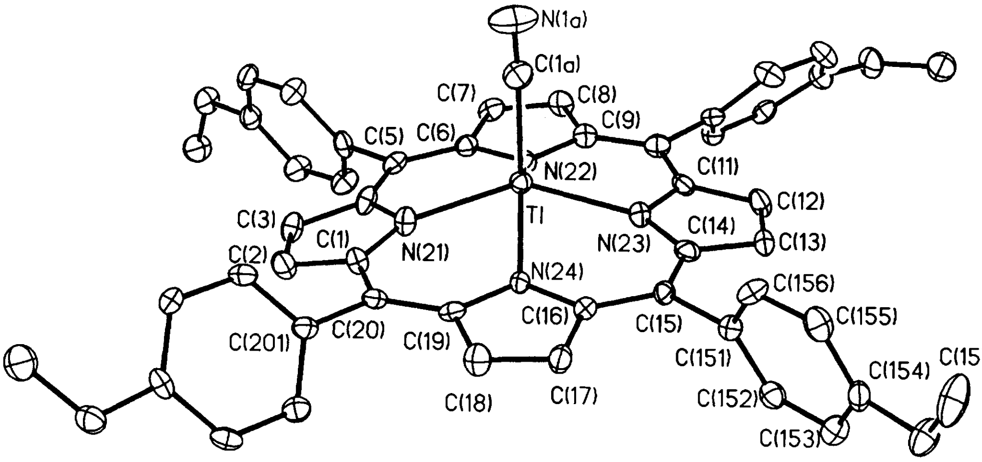

Fig. 5 Computer-generated plot and numbering scheme of [Tl(tmpp)(CN)]. The figure shows cyanide binding. For a discussion of CN *versus* NC binding see text

83.5° respectively with regard to the 4N plane. The Tl–S bond lengths are 2.527(2) and 2.552(2) Å. The only other thallium(III) thiocyanate compound we found, [$TlMe_2(SCN)$],[45] forms infinite layers with octahedral co-ordination of the Tl and is thus not directly comparable. A monomeric thallium(III) compound with a Tl–S bond is (diethyldithiocarbamato)-diphenylthallium(III),[31c] which has bidentate S-bonding and exhibits therefore longer Tl–S bond lengths (2.72 Å) than observed here. The SCN group is almost linear with S–C–N angles of 177.3(9) and 177.9(7)° in both porphyrin molecules. The bond lengths within the ligand are 1.687(6) and 1.689(6) Å for the sulfur–carbon bond and 1.128(9) and 1.145(9) Å for the carbon–nitrogen bond. These values agree well with the reverse order found in the isothiocyanato ligand of some other metalloporphyrins.[46] Thus there is no ambiguity with regard to SCN *versus* NCS binding. Refinement for the latter possibility gave obviously wrong thermal parameters and showed that the initial refinement as thiocyanate was correct.

A similarly bent ligand was found in the structures of two thallium(III) azide porphyrins. Fig. 8 shows the molecular structure of [Tl(tpp)(N_3)]. The corresponding compound [Tl(tmpp)(N_3)] crystallizes with one methylene chloride solvate molecule in the asymmetric unit. The orientation of the axial ligand with regard to the macrocycle is rather similar to that found in the thiocyanate ligand. The N–N–N vector is tilted by 78.4° from the 4N plane in [Tl(tpp)(N_3)] and by 86.8° in [Tl(tmpp)(N_3)]. The Tl–N(1)–N(2) angles are comparable in the two compounds, 111.6(7) and 112.6(6)°. This makes the azide ligand less bent than the thiocyanate ligand, which exhibited angles of $\approx 96°$ (see above). The N–N bond lengths within the axial ligand are 1.210 Å for N(1)–N(2) and slightly shorter for the terminal N(2)–N(3) bond, 1.167(11) and 1.139(7) Å. The azide ligand is almost linear with an N–N–N angles of 176.4(9)° in [Tl(tmpp)(N_3)] and 176.7(12)° in [Tl(tpp)(N_3)]. The Tl–N(porphyrin)–N_{ax} system deviates from a perfect square-pyramidal co-ordination. The smallest such angle is 102.0(2)° for N(1)–Tl–N(24) in [Tl(tpp)(N_3)] while the largest is 115.3(2)° for N(1)–Tl–N(22). In [Tl(tmpp)(N_3)] these angles are 99.1(2) and 117.8(2)°, respectively. The structural parameters of the azide ligand compare reasonably well with those of other metalloporphyrin azide complexes. In [{Mn^{IV}(tpp)-(N_3)}$_2$O][47a] N–N bond lengths of 1.06(1) and 1.15(1) Å and a N–N–N bond angle of 176.9(14)° is observed. Similar values have been found in [Fe^{III}(tpp)(N_3)(py)][47b] (py = pyridine) which exhibits an Fe–N–N angle of 125.6(7)°.

The Tl–N(porphyrin) and Tl–N_{ax} bond lengths are identical in these five-co-ordinate thallium(III) complexes, 2.218(4) and 2.202(9) in [Tl(tpp)(N_3)] and 2.204(4) and 2.205(6) Å in

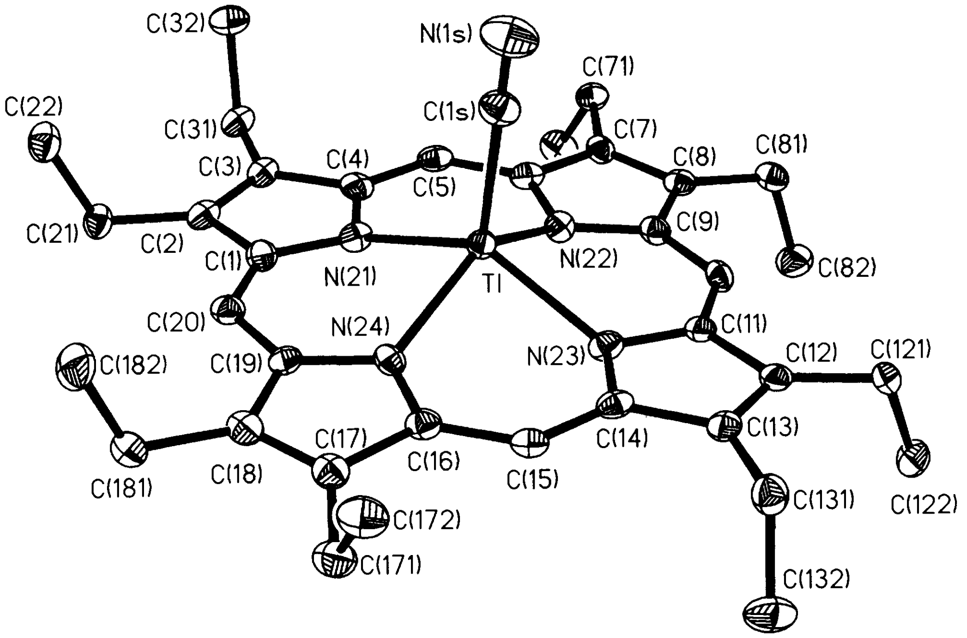

Fig. 6 Computer-generated plot and numbering scheme of $[\mathrm{Tl(oep)(CN)}]$

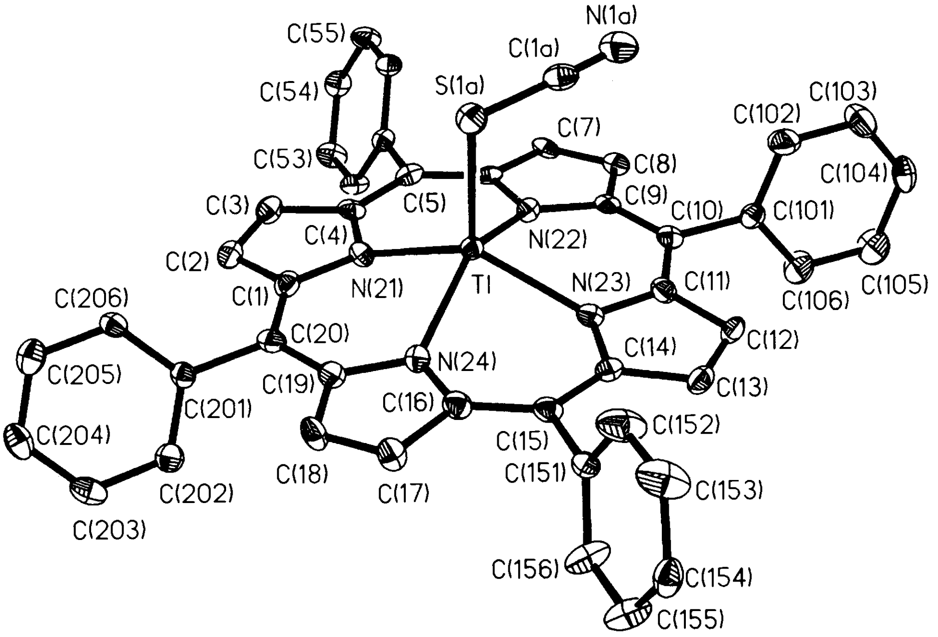

Fig. 7 Computer-generated plot and numbering scheme of $[\mathrm{Tl(tpp)(SCN)}]$

$[\mathrm{Tl(tmpp)(N_3)}]$. In six-co-ordinated complexes considerable differences were found between the equatorial and axial bond lengths, the former being about 2.1–2.2 Å and the latter considerably longer in the range 2.4–2.5 Å.[39e,43a,b,48a] In trichloro(1,10-phenanthroline)thallium(III) which has a five-co-ordinated thallium centre, Tl–N distances of 2.364(8) Å were found.[34] Much shorter bond lengths of 2.089(18) Å were found in a complex with three-co-ordinated thallium, $\mathrm{Tl[N(SiMe_3)_2]_3}$.[36b]

Thallium stereochemistry. The Tl–X distances agree well with those observed in 'smaller' molecules and, as expected, increase in the series F < Cl < Br < I. All distances determined here were found to agree well with terminal lengths found in other $\mathrm{Tl^{III}X}$ compounds. Note that the Tl–F distance observed in $[\mathrm{Tl(tpp)F}]$ [2.441(6) Å][19] lies at the upper limit of the distance observed in *e.g.* $\mathrm{TlF_3}$[49a] or $\mathrm{K[TlF_4]}$.[49b] A similar trend is observed when, *e.g.* the M–Cl distances in the main-group III porphyrins are compared. The bond distance between metal centre and the axial ligand increases in the series $\mathrm{Ga^{III}}$ (2.196 Å),[6] $\mathrm{In^{III}}$ (2.369 Å),[8] and $\mathrm{Tl^{III}}$ (see Table 4). The Tl–N(porphyrin) distances do not vary much with the nature of the axial ligand, in general being of the order of 2.20–2.24 Å. A slight increase in this distance can be observed in the halogeno series.

Five-co-ordinated main-group porphyrins differ in one important aspect from transition-metal complexes. A large variation in co-ordination group geometry is observed as a function of the axial ligand.[1] The best characteristic for this is the displacement of the central metal from the 4N plane. Table 5 shows that the M–N(porphyrin) distance in main-group porphyrins correlates roughly with the displacement of the metal. It was pointed out by Scheidt and Lee[1] and Guilard *et al.*[33e] that considerable differences occur between the displacements in main-group and transition-metal complexes with σ-bonded axial ligands. Main-group complexes with such

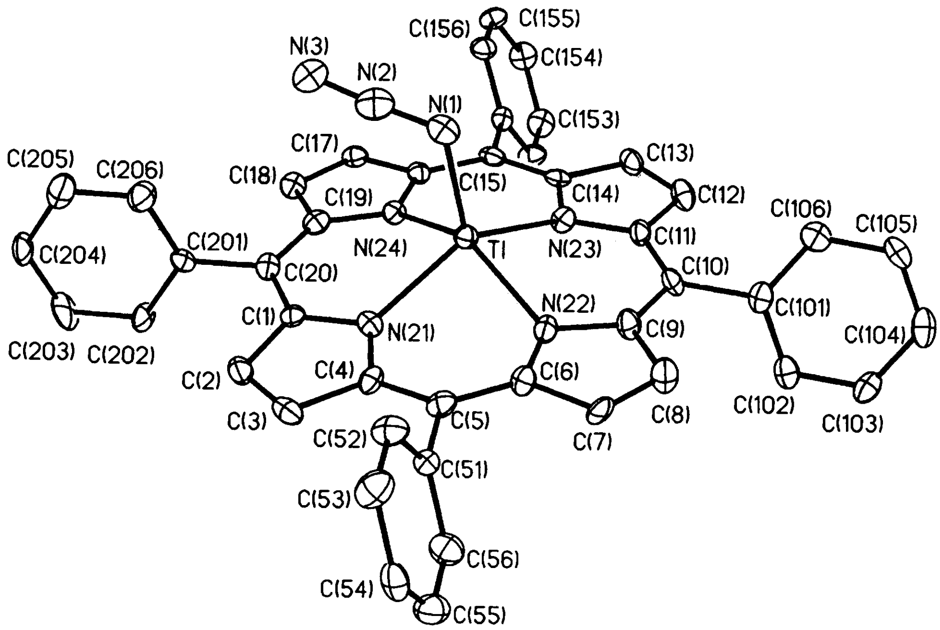

Fig. 8 Computer-generated plot and numbering scheme of [Tl(tpp)(N_3)]

Table 4 Stereochemical parameters (Å) for main-group III porphyrin complexes

Compound	M–N(porphyrin)	M–L_{ax}	Δ4N	Δ24	Ref.
[Al(oep)Me]	2.033(3)	1.942(3)	0.47	0.53	4
[Ga(oep)(OSO_2Me)]	2.013(5)	1.908(6)	0.32	0.33	5
[Ga(tpp)Cl]	2.021(1)	2.196(2)	0.32	0.32	6
[Ga(oep)(N_3)]	2.030	1.955(2)	0.36	0.40	7
[In(oep)(N_4CPh)]	2.128(4)	2.183(5)	0.46	0.49	9(*a*)
[In(oep)(N_4CMe)]	2.135(7)	2.177(6)	0.49	0.49	9(*b*)
[In(tpp)Cl]	2.156(6)	2.369(2)	0.61	0.71	8
[In(oep)][Mn($CO)_5$]	2.193(4)	2.705(1)	0.74	0.81	10(*a*)
[In(tpp)Me]	2.20(1)	2.13(1)	0.78	0.92	11
[In(oep)][Mo(η-C_5H_5)($CO)_3$]	2.201(2)	2.890(1)	0.79	0.86	10(*b*)
[TlL^1(Cl)]	2.204(9)	2.487(4)	0.66	0.75	This work
[Tl(tmpp)Cl]	2.206(5)	2.451(2)	0.72	0.82	This work
[Tl(oep)Cl]	2.212(6)	2.499(3)	0.69	0.75	12
[Tl(tpp)Cl]	2.21(1)	2.420(4)	0.62	0.74	13
[Tl(tpp)(SCN)]	2.208(3)	2.527(2)	0.72	0.80	This work
[Tl(tmpp)(SCN)]	2.210(3)	2.552(2)	0.73	0.83	This work
[Tl(tpp)F]	2.213(13)	2.441(6)	n.d.	0.74	19
[TlL^2(O_2CMe)]	2.217(6)	2.388(7)	0.73	0.77	This work
[TlL^1(O_2CMe)]	2.219(3)	2.394(7)	0.74	0.88	This work
[Tl(tpp)(O_2CMe)]	2.219(7)	2.33(1)	—	0.84	18
[Tl(tmpp)N_3)]	2.204(4)	2.205(6)	0.71	0.78	This work
[Tl(tpp)(N_3)]	2.218(4)	2.202(9)	0.73	0.82	This work
[Tl(tmpp)(CN)]	2.218(5)	2.193(7)	0.76	0.86	This work
[Tl(oep)(CN)]	2.220(4)	2.215(8)	0.76	0.79	This work
[Tl(tpp)(NC)]	2.222(10)	2.260(3)	0.77	0.91	20
[Tl(tpp)Br]	2.231(6)	2.542(2)	0.76	0.88	This work
[Tl(tmpp)I]	2.220(5)	2.727(1)	0.79	0.84	This work
[Tl(tpp)I]	2.237(5)	2.714(4)	0.81	0.91	This work
[Tl(tpp)Me]	2.29(1)	2.147(12)	0.84	0.98	13
[Tl(tpp)(nor)] *	2.29	2.09	0.99	1.10	14
[Tl(oep)][Mn($CO)_5$]	2.264(5)	2.649(1)	0.94	0.98	15
[Tl(oep)][Mo(η-C_5H_5)($CO)_3$]	2.294(5)	2.829(1)	1.00	1.06	16

* nor = norbornyl

ligands, *e.g.* [Tl(tpp)Me], show significantly larger displacements than those of the halogeno complexes. Using the mean values for compounds with identical axial ligands the following series of displacements from the 4N plane were observed: Cl, 0.67; Br, 0.76; I, 0.8; N_3, 0.72; SCN, 0.73; CN/NC, 0.76 Å. A similar increase in the halogeno series and ordering of the pseudohalogeno compounds between Cl and Br is obtained for the displacements from the 24-core-atom plane: F, 0.74; Cl, 0.77; Br, 0.88; I, 0.88; N_3, 0.8; SCN, 0.82; CN/NC, 0.85 Å. The ordering in the halogeno series correlates with increasing covalent character of the metal–ligand bond.

The large thallium atom leads also to a significant expansion of the macrocycle core. Collins and Hoard[50] estimated the optimum size of the co-ordination hole (the space between diagonally opposite pyrrole nitrogens) to be 4.02 Å (distance, Ct–N, from the geometrical centre of the 4N plane to the nitrogens is 2.01 Å). We have determined the Ct–N distances for structurally characterized compounds in order to test any

Table 5 Comparison of the porphyrin core-ruffling effect in the structures studied. Numbers refer to the deviations (Å) of equivalent atoms from the least-squares plane of the 24 core atoms. Deviations from the least-squares plane of the four nitrogen atoms in parentheses

Compound	24 atom *	C_m	C_a	C_b
[TlL^1(Cl)]	0.08	0.11 (0.11)	0.06 (0.08)	0.08 (0.17)
[Tl(tmpp)Cl]	0.10	0.09 (0.04)	0.06 (0.08)	0.26 (0.22)
[Tl(tpp)(SCN)]	0.06	0.05 (0.11)	0.04 (0.08)	0.08 (0.18)
[Tl(tmpp)(SCN)]	0.14	0.05 (0.05)	0.08 (0.11)	0.25 (0.31)
[TlL^1(O$_2$CMe)]	0.12	0.15 (0.09)	0.09 (0.11)	0.13 (0.27)
[TlL^2(O$_2$CMe)]	0.08	0.03 (0.03)	0.03 (0.05)	0.10 (0.15)
[Tl(tpp)(N$_3$)]	0.06	0.05 (0.06)	0.04 (0.08)	0.09 (0.19)
[Tl(tmpp)(N$_3$)]	0.09	0.07 (0.07)	0.08 (0.08)	0.10 (0.21)
[Tl(tmpp)(CN)]	0.09	0.06 (0.08)	0.05 (0.08)	0.13 (0.21)
[Tl(oep)(CN)]	0.04	0.03 (0.03)	0.03 (0.03)	0.06 (0.11)
[Tl(tpp)Br]	0.07	0.01 (0.12)	0.04 (0.09)	0.10 (0.19)
[Tl(tpp)I]	0.06	0.01 (0.04)	0.03 (0.07)	0.09 (0.18)
[Tl(tmpp)I]	0.06	0.06 (0.11)	0.04 (0.08)	0.09 (0.13)

* Average deviations of the 24 core atoms from their least-squares plane.

influence of the axial ligand on the core size. On average for the different Tl–X systems the Ct–N distances were: MeCO$_2$, 2.094; Cl, 2.095; Br, 2.097; I, 2.08, CN/NC, 2.085; N$_3$, 2.09; and SCN, 2.086 Å. Thus, there is no correlation between the core size and the axial ligand. The average Ct–N distance for all thallium porphyrins studied is 2.09 Å. Slightly larger cores are observed in [TlL(Cl)] (L = 5,15-dioxo [17] or 5,10,15,20-tetranitro [38] oep derivative), with Ct–N 2.12 and 2.11 Å. The former compound is not formally a porphyrin and has two oxidized *meso*-groups which allow for more flexibility in the macrocycle, and the latter compound is a dodecasubstituted, sterically 'overloaded' porphyrin, which relieves part of the strain imposed by the substituents *via* in-plane distortion and core expansion.

Macrocycle conformation. The acetato complexes with a six-co-ordinated thallium do not differ appreciably in their bond length and angle characteristics from those of the five-co-ordinated species. Also the displacement characteristics of the thallium are comparable to those found for the pseudohalogeno complexes. In general no significant differences were observed for the structural characteristics of the macrocycle in the different porphyrin series. The bond lengths and angles (Table 3) agree well with those described for other thallium(III) porphyrins and do not vary significantly with alterations in the axial ligand.[12–18] The only differences can be found in the structure of the 5,10,15,20-tetranitro derivative of oep, a dodecasubstituted porphyrin,[38] which exhibits slightly longer C_a–C_m bond lengths.

The large thallium atom induces considerable conformational distortion in the macrocycle.[12,13] This type of distortion observed in a variety of metalloporphyrins with large metal ions [1] has been described as 'doming'. Tables 3 and 4 summarize some of the parameters which can be used to describe the conformational behaviour of these porphyrins. The difference between the displacement of the metal centre from the 4N plane (Δ4N) and from the plane of the macrocycle atoms (Δ24), which is zero for a planar macrocycle, has been used to describe the degree of doming. The thallium porphyrins show generally a difference of Δ24 − Δ4N of 0.06–0.14 Å. The largest such difference is observed for [Tl(tpp)(NC)].[20] These values do not however, always correlate with the average displacement of the macrocycle atoms from their least-squares plane (Table 5). For example, both [Tl(tpp)I] and [Tl(tmpp)I] have average displacements of the macrocycle atoms of 0.06 Å, but their Δ24 − Δ4N values are 0.10 and 0.05 Å, respectively. Other parameters useful for determining the degree of distortion are the displacement values for the C_m, C_a and C_b atoms (for definition see Table 3). The average deviations of equivalent atoms are listed in Table 5. Considerable differences occur from case to case, even in porphyrins with the same axial ligand, *e.g.* as observed for the two Tl(SCN) porphyrins. The average values listed in Table 5 are actually somewhat misleading since single atoms can exhibit much larger displacements. The largest such distortions observed in the porphyrin series described here are 0.42 and 0.47 Å for C(2) and C(3) in [Tl(tmpp)(CN)] and 0.56 Å for C(12) and C(13) in [Tl(tmpp)(SCN)]. Clearly, there is no correlation between the type of axial ligand and the degree of distortion; nor is there a correlation with the thallium displacements. Even when systems with much larger thallium displacements are considered, *e.g.* [Tl(tpp)Me], no such correlation can be made. Thus the reason for the sometimes considerable differences in displacements and conformation remains unclear.

Molecular Packing.—The [Tl(tpp)X] porphyrin series with X = F, Cl, Br and I is an example of an isostructural series. All compounds crystallize in the monoclinic space group $P2_1/n$ with a cell volume of roughly 3450 Å^3. Although the overall cell constants are similar, the situation is different in the case of the tmpp series, probably due to the flexible orientation of the *p*-methoxy groups. The large porphyrin–porphyrin separation in the crystal and the rather similar packing are also responsible for the fact that [Tl(tpp)(CN)] can also be integrated into the isomorphous [Tl(tpp)X] crystal series with similar cell constants. The complexes [Tl(tpp)(SCN)] and [Tl(tpp)(N$_3$)] can also be considered to be homotypes. Overall the five-co-ordinate thallium(III) porphyrins in each given ligand system show very similar crystal packing and roughly the same cell volume.

The thallium displacements in the above-mentioned compounds are not due to packing constraints. Considerable differences in displacements are observed in the isostructural series [Tl(tpp)X], with X = Me, F, Cl, Br, I or between [In(tpp)Me] and [In(tpp)Cl]. The isostructural relationships also show that the macrocycle deformations observed in the different compounds are not due to packing constraints and intermolecular interactions.

Fig. 9 shows an example of the molecular packing of a coproporphyrin derivative, [TlL^1(Cl)]. The axial ligands of neighbouring metalloporphyrins point towards each other into the void between the macrocycles. In this case the intermolecular space is also filled with the methylene chloride molecules of solvation. The longer propionic methyl ester side chains of the macrocycle give the molecular a 'chair-like' shape by pairwise pointing away from the macrocycle in opposite directions. Close contacts were observed between the propionic ester side chain and the solvent molecules: O(3) ··· Cl(1S) 3.12 Å and O(4) ··· Cl(1S) 3.02 Å. Similarly in the structure of [TlL^1(O$_2$CMe)] a contact of 3.1 Å was observed between O(7) of an ester side chain and Cl(2S) of the solvent molecules. This packing is typical for all coproporphyrin complexes studied here.

Fig. 10 shows the molecular packing of [Tl(tpp)(CN)] as an example for a *meso*-tetraphenylporphyrin. Again, in all cases orientation of the axial ligands in opposite direction in neighbouring molecules is observed. The molecules thus pack in layers of macrocycles with alternating orientation of the axial ligands. In the case of the tmpp series the same general type of packing was observed. All packing patterns agree well with the general scheme deduced for such porphyrins by Strouse and co-workers.[51]

With the exception of the above-mentioned side chain–solvent molecule interactions no unusually short intermolecular contacts were observed. This is further indication that the observed macrocycle conformations are intrinsic properties of the metalloporphyrin system which do not arise from packing constants. Significant conformational distortions have been observed in π-stacked dimers due to the general tendency of metalloporphyrins for aggregation.[1,52] No close aggregation is observed in the structures of the tpp and tmpp series. In the

Table 6 Atomic coordinates (× 10^4) for $[TlL^1(O_2CMe)]\cdot CH_2Cl_2$

Atom	*x*	*y*	*z*
Tl	1449(1)	566(1)	1346(1)
C(1a)	1327(4)	2491(5)	1823(4)
C(2a)	1317(6)	3530(5)	2054(5)
O(1a)	489(5)	2202(4)	2291(4)
O(2a)	2243(5)	1872(4)	1181(4)
N(21)	−12(3)	1041(3)	759(3)
N(22)	2684(3)	134(3)	−281(2)
N(23)	2869(3)	−873(3)	1664(2)
N(24)	194(2)	33(3)	2693(2)
C(1)	−1221(3)	1367(4)	1368(4)
C(2)	−1917(5)	1872(4)	719(4)
C(21)	−3259(5)	2323(4)	1080(5)
C(22)	−3830(5)	3508(5)	1307(5)
C(23)	−5192(6)	3963(5)	1656(5)
C(24)	−6989(6)	5450(6)	2388(6)
C(3)	−1097(5)	1834(4)	−262(4)
C(31)	−1375(6)	2269(5)	−1206(4)
C(4)	104(5)	1317(4)	−242(3)
C(5)	1199(5)	1104(4)	−1082(4)
C(6)	2369(5)	573(4)	−1112(3)
C(7)	3479(5)	319(4)	−2036(4)
C(71)	3534(5)	636(5)	−3116(4)
C(72)	3731(6)	1663(5)	−3433(4)
C(73)	3877(5)	1945(5)	−4537(4)
C(74)	3981(7)	3289(6)	−5780(5)
C(8)	4419(5)	−246(4)	−1727(4)
C(81)	5747(5)	−715(5)	−2393(4)
C(9)	3922(3)	−366(4)	−620(4)
C(10)	4547(5)	−968(4)	2(4)
C(11)	4075(3)	−1241(4)	1035(4)
C(12)	4758(5)	−2028(4)	1591(4)
C(121)	6107(5)	−2647(4)	1200(5)
C(122)	6500(6)	−3756(5)	801(5)
C(123)	7697(6)	−4506(5)	877(5)
C(124)	9422(6)	−6107(5)	222(7)
C(13)	3951(5)	−2147(4)	2529(4)
C(131)	4204(5)	−2929(5)	3350(4)
C(14)	2748(5)	−1411(4)	2580(2)
C(15)	1651(5)	−1285(4)	3391(4)
C(16)	469(5)	−626(3)	3466(3)
C(17)	−639(5)	−526(4)	4335(4)
C(171)	−750(5)	−1182(4)	5302(4)
C(172)	−1293(6)	−1971(5)	5349(4)
C(173)	−566(6)	−2760(5)	4468(6)
C(174)	−634(9)	−3924(8)	3477(9)
C(18)	−1569(5)	219(4)	4088(4)
C(181)	−2894(5)	648(5)	4759(4)
C(19)	−1045(2)	541(4)	3041(4)
C(20)	−1675(5)	1175(4)	2425(4)
O(1)	−5688(4)	4941(3)	2018(4)
O(2)	−5775(4)	3503(4)	1651(5)
O(3)	3872(4)	2930(3)	−4741(3)
O(4)	4015(4)	1373(3)	−5160(3)
O(5)	8310(4)	−5275(3)	157(4)
O(6)	8064(5)	−4454(4)	1509(4)
O(7)	469(5)	−3024(4)	3948(4)
O(8)	−1256(5)	−3099(5)	4266(6)

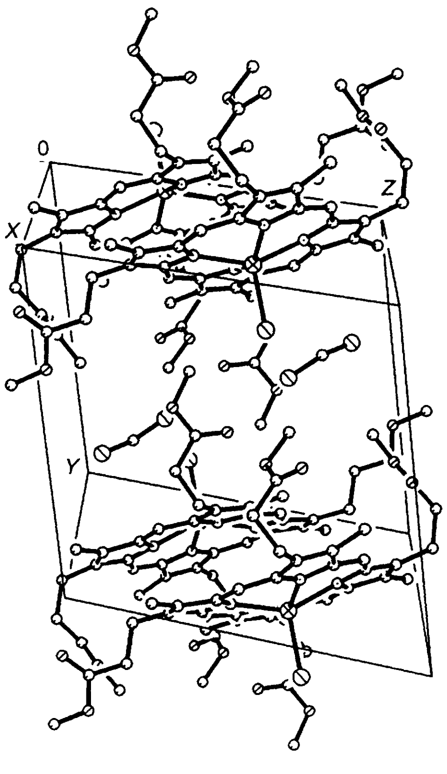

Fig. 9 View of the molecular packing in the unit cell of $[TlL^1(Cl)]$. Hydrogen atoms have been omitted for clarity

coproporphyrin derivatives weakly bonded dimers can be observed. On the basis of the classification given by Scheidt and Lee[1] for such systems we determined the mean plane separation, the centre-to-centre distance (Ct–Ct) and the lateral shift of the centres [defined as sin(slip angle) × Ct–Ct]. In $[TlL^1(Cl)]$ the plane separation was 3.543 Å and the lateral shift of the centres 4.76 Å. In $[TlL^1(O_2CMe)]$ these values were 3.71 Å and 4.92 Å, while for $[TlL^2(O_2CMe)]$ a mean plane separation of 3.59 Å and a lateral shift of 4.98 Å were determined. According to the classification given by Scheidt and Lee[1] these values place the dimeric aggregates into the upper region of weak interactions. Thus, aggregation phenomena can also be excluded with regard to the conformation distortion observed in the thallium compounds.

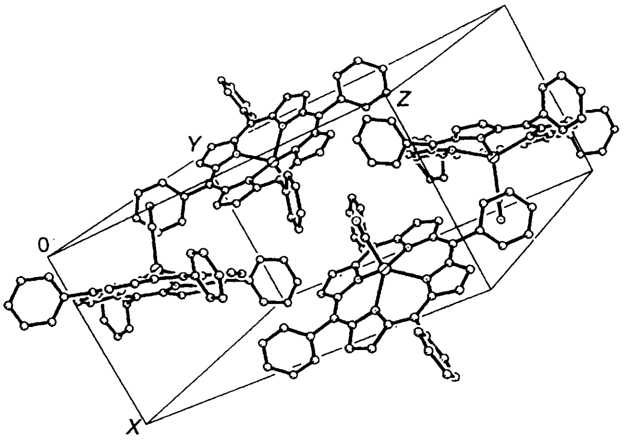

Fig. 10 View of the molecular packing in the unit cell of [Tl(tpp)(CN)]

Conclusions

This study has shown that by simple ligand-exchange reactions the complete halogeno series of thallium porphyrins can be prepared and that this method can be extended to pseudohalogens. The stereochemistry of thallium bromide, iodide, azide and isothiocyanate porphyrins was elucidated. The N_3 and SCN complexes show a bent orientation of the ligand with regard to the porphyrin and the acetate ligands binds in a symmetric bidentate fashion. All (pseudo)halogeno complexes have a five-co-ordinated thallium(III) centre with considerable

Table 7 Atomic coordinates (× 10^4) for [$TlL^2(O_2CMe)$]

Atom	*x*	*y*	*z*	Atom	*x*	*y*	*z*
Tl	1958(1)	485(1)	2279(1)	C(11)	2610(5)	861(3)	70(5)
C(1a)	2169(5)	1351(3)	3626(6)	C(12)	3533(5)	972(3)	−316(5)
C(2a)	2386(7)	1813(2)	4488(7)	C(121)	3583(6)	1274(3)	−1349(6)
O(1a)	2927(5)	1145(2)	3410(5)	C(122)	3749(7)	1873(3)	−1177(6)
O(2a)	1295(5)	1216(3)	3237(5)	C(123)	3933(6)	2152(3)	−2194(6)
N(21)	899(4)	−71(2)	2846(5)	C(124)	4061(8)	3010(3)	−3015(8)
N(22)	658(4)	608(2)	802(4)	C(13)	4347(5)	748(3)	445(6)
N(23)	2888(4)	572(2)	1032(4)	C(131)	5474(6)	746(3)	439(7)
N(24)	3124(4)	−134(2)	3033(4)	C(14)	3941(5)	482(3)	1286(6)
C(1)	1163(5)	−395(2)	3751(5)	C(15)	4490(5)	171(3)	2186(6)
C(2)	235(5)	−547(2)	4081(6)	C(16)	4138(5)	−118(3)	2981(6)
C(21)	204(6)	−906(3)	5048(5)	C(17)	4746(5)	−466(3)	3821(6)
C(22)	381(6)	−1513(3)	4886(6)	C(171)	5878(5)	−560(3)	4021(6)
C(23)	−481(6)	−1795(3)	4061(6)	C(18)	4092(5)	−683(3)	4406(6)
C(24)	−1178(7)	−2633(3)	3511(8)	C(181)	4311(6)	−1077(3)	5327(6)
C(3)	−575(5)	−303(3)	3356(5)	C(182)	4044(7)	−1656(3)	4935(9)
C(31)	−1701(5)	−314(3)	3357(6)	C(183)	3628(7)	−1996(4)	5803(9)
C(4)	−150(5)	−2(3)	2569(6)	C(184)	3404(10)	−2823(5)	6481(12)
C(5)	−719(5)	281(3)	1647(6)	C(19)	3066(5)	−471(3)	3896(5)
C(6)	−360(5)	554(2)	847(6)	C(20)	2162(5)	−572(2)	4229(6)
C(7)	−1000(5)	814(2)	−151(5)	O(1)	−1143(4)	−1596(2)	3352(5)
C(71)	−2166(5)	828(3)	−433(6)	O(2)	−394(4)	−2338(2)	4235(5)
C(8)	−366(5)	1021(3)	−741(5)	O(3)	−1748(5)	2144(2)	−3309(5)
C(81)	−657(5)	1342(3)	−1780(5)	O(4)	−784(6)	2810(2)	−2344(5)
C(82)	−520(6)	1952(3)	−1566(6)	O(5)	4133(5)	1934(2)	−2963(5)
C(83)	−1098(7)	2295(3)	−2528(6)	O(6)	3858(4)	2689(2)	−2113(4)
C(84)	−1305(10)	3193(4)	−3176(9)	O(7)	3194(8)	−1787(4)	6410(9)
C(9)	699(5)	892(3)	−130(5)	O(8)	3829(5)	−2499(3)	5707(8)
C(10)	1599(5)	1008(3)	−454(6)				

Table 8 Atomic coordinates (× 10^4) for [Tl(tmpp)Cl]

Atom	*x*	*y*	*z*	Atom	*x*	*y*	*z*
Tl	1 760(1)	3 511(1)	2 689(1)	C(107)	5 479(7)	10 983(6)	1 172(6)
Cl	3 214(2)	2 113(2)	2 641(1)	C(11)	3 119(6)	6 022(5)	3 049(5)
N(21)	139(5)	2 642(4)	1 948(4)	C(12)	3 597(6)	6 887(6)	3 780(5)
N(22)	1 782(5)	4 402(5)	1 453(4)	C(13)	3 316(6)	6 554(6)	4 591(5)
N(23)	2 524(5)	5 169(5)	3 436(4)	C(14)	2 657(6)	5 453(5)	4 376(4)
N(24)	854(5)	3 431(5)	3 943(3)	C(15)	2 160(5)	4 846(5)	5 034(4)
C(1)	−628(5)	1 945(5)	2 344(4)	C(151)	2 601(6)	5 226(5)	6 011(4)
C(2)	−1 413(6)	1 331(6)	1 610(5)	C(152)	3 770(6)	5 301(6)	6 286(5)
C(3)	−1 117(5)	1 638(5)	792(4)	C(153)	4 233(6)	5 660(6)	7 197(5)
C(4)	−114(6)	2 446(5)	1 003(4)	C(154)	3 501(6)	5 954(5)	7 858(4)
C(5)	501(6)	2 983(5)	358(4)	C(155)	2 310(6)	5 880(5)	7 607(4)
C(51)	132(6)	2 576(6)	−636(4)	C(156)	1 861(6)	5 520(5)	6 701(4)
C(52)	41(7)	1 395(6)	−970(5)	C(157)	5 036(6)	6 328(7)	9 075(5)
C(53)	−399(7)	981(6)	−1 870(5)	C(16)	1 298(6)	3 916(5)	4 821(4)
C(54)	−733(7)	1 741(6)	−2 457(5)	C(17)	675(6)	3 351(5)	5 473(4)
C(55)	−581(6)	2 924(6)	−2 168(4)	C(18)	−117(6)	2 573(6)	4 989(5)
C(56)	−178(6)	3 325(5)	−1 263(4)	C(19)	−5(6)	2 586(5)	4 022(5)
C(57)	−1 966(7)	370(7)	−3 494(5)	C(20)	−687(5)	1 907(5)	3 287(4)
C(6)	1 374(6)	3 885(5)	565(4)	C(201)	−1 585(6)	1 062(6)	3 542(4)
C(7)	1 967(6)	4 459(6)	−80(5)	C(202)	−1 252(6)	62(6)	3 856(5)
C(8)	2 678(6)	5 337(6)	404(5)	C(203)	−2 067(7)	−723(6)	4 121(5)
C(9)	2 578(5)	5 296(5)	1 368(4)	C(204)	−3 200(6)	−503(6)	4 092(5)
C(10)	3 180(6)	6 054(6)	2 101(4)	C(205)	−3 550(6)	480(6)	3 768(5)
C(101)	3 915(6)	7 038(5)	1 849(4)	C(206)	−2 746(6)	1 258(6)	3 492(5)
C(102)	3 411(6)	7 906(6)	1 447(5)	C(207)	−3 680(8)	−2 175(8)	4 774(7)
C(103)	4 056(6)	8 884(6)	1 276(5)	O(1)	−1 225(5)	1 410(4)	−3 352(3)
C(104)	5 246(6)	8 947(6)	1 458(5)	O(2)	5 978(5)	9 855(4)	1 288(4)
C(105)	5 773(6)	8 075(6)	1 832(5)	O(3)	3 837(4)	6 353(4)	8 766(3)
C(106)	5 101(6)	7 127(6)	2 021(5)	O(4)	−4 059(5)	−1 194(4)	4 388(4)

displacement of the thallium atoms from the 4N plane. The displacement of the thallium could be correlated with the covalent character of the metal–ligand bond. No correlation of the axial ligand type was possible with the degree and type of macrocycle distortion induced by the large thallium atom.

Experimental

General.—All chemicals were of analytical grade and obtained from Aldrich Chemical Co. Melting points were determined with a Mel-temp II apparatus (Laboratory Instruments) and are uncorrected. Elemental analyses were performed

Table 9 Atomic coordinates (× 10^4) for $[TlL^1(Cl)]\cdot CH_2Cl_2$

Atom	*x*	*y*	*z*
Tl	3 427(1)	9 531(1)	3 762(1)
Cl	2 589(3)	7 979(2)	3 566(2)
N(21)	2 387(8)	9 825(7)	5 373(6)
N(22)	2 445(7)	10 959(7)	3 319(6)
N(23)	4 895(8)	10 046(7)	2 304(6)
N(24)	4 845(8)	8 914(7)	4 351(6)
C(1)	2 580(10)	9 326(9)	6 237(7)
C(2)	1 556(11)	9 531(9)	7 139(7)
C(21)	1 372(11)	9 062(8)	8 253(7)
C(22)	911(12)	7 981(8)	8 520(7)
C(23)	570(11)	7 528(8)	9 659(7)
C(24)	186(18)	5 947(14)	10 838(9)
C(3)	760(12)	10 138(10)	6 804(9)
C(31)	−459(12)	10 595(12)	7 448(9)
C(4)	1 289(9)	10 335(9)	5 684(9)
C(5)	813(11)	10 989(11)	5 010(9)
C(6)	1 354(8)	11 331(9)	3 937(8)
C(7)	890(9)	12 129(9)	3 325(9)
C(71)	−278(9)	12 776(8)	3 738(9)
C(72)	−235(11)	13 610(8)	4 352(8)
C(73)	568(10)	14 451(8)	3 654(8)
C(74)	2 341(14)	15 239(12)	3 211(11)
C(8)	1 735(11)	12 271(10)	2 338(9)
C(81)	1 758(12)	13 067(10)	1 402(9)
C(9)	2 706(11)	11 484(9)	2 338(7)
C(10)	3 771(11)	11 370(10)	1 483(9)
C(11)	4 786(11)	10 692(8)	1 465(7)
C(12)	5 865(11)	10 591(9)	560(7)
C(121)	6 135(11)	11 199(8)	−521(7)
C(122)	6 908(10)	12 094(7)	−743(9)
C(123)	6 247(10)	12 998(9)	−142(9)
C(124)	6 296(17)	14 239(12)	860(14)
C(13)	6 601(11)	9 842(10)	883(9)
C(131)	7 800(11)	9 413(10)	230(9)
C(14)	5 987(9)	9 524(9)	2 004(9)
C(15)	6 438(11)	8 840(10)	2 661(9)
C(16)	5 949(8)	8 567(9)	3 735(9)
C(17)	6 470(9)	7 906(9)	4 420(9)
C(171)	7 707(10)	7 369(9)	4 026(10)
C(172)	7 815(11)	6 451(8)	3 452(9)
C(173)	7 127(11)	5 528(8)	4 116(9)
C(174)	6 635(14)	3 843(10)	4 097(13)
C(18)	5 710(11)	7 900(9)	5 407(9)
C(181)	5 837(12)	7 331(10)	6 390(9)
C(19)	4 658(11)	8 543(9)	5 365(7)
C(20)	3 635(11)	8 734(10)	6 213(9)
O(1)	485(9)	6 483(7)	9 782(6)
O(2)	408(8)	8 029(7)	10 349(6)
O(3)	7 299(9)	4 747(7)	3 540(8)
O(4)	6 501(9)	5 483(8)	5 020(7)
O(5)	419(8)	14 979(7)	2 917(6)
O(6)	1 507(8)	14 498(7)	3 913(7)
O(7)	5 278(9)	13 374(8)	−80(8)
O(8)	6 866(9)	13 324(8)	343(8)

Table 10 Atomic coordinates (× 10^4) for [Tl(tpp)Br]

Atom	*x*	*y*	*z*
Tl	3332(1)	1834(1)	1538(1)
Br	1012(1)	2452(1)	1756(1)
N(21)	3491(7)	1379(4)	555(3)
N(22)	3244(7)	491(3)	1748(3)
N(23)	4598(6)	1881(4)	2402(2)
N(24)	4759(7)	2813(3)	1215(3)
C(1)	3755(7)	1907(5)	50(3)
C(2)	3362(8)	1465(5)	−504(3)
C(3)	2891(9)	720(5)	−341(3)
C(4)	2968(8)	668(5)	336(3)
C(5)	2630(8)	−33(5)	696(3)
C(51)	2073(9)	−752(4)	341(3)
C(52)	2888(9)	−1141(5)	−115(3)
C(53)	2371(9)	−1793(5)	−468(3)
C(54)	1082(10)	−2066(5)	−353(4)
C(55)	287(9)	−1695(5)	94(4)
C(56)	781(8)	−1045(5)	442(3)
C(6)	2791(8)	−105(4)	1344(3)
C(7)	2583(9)	−861(5)	1701(3)
C(8)	2934(8)	−689(4)	2312(3)
C(9)	3345(8)	159(4)	2336(3)
C(10)	3895(8)	547(4)	2867(3)
C(101)	4010(9)	57(4)	3463(3)
C(102)	2850(10)	−132(5)	3815(3)
C(103)	2979(10)	−575(5)	4370(3)
C(104)	4214(10)	−837(5)	4566(3)
C(105)	5374(10)	−664(5)	4223(3)
C(106)	5238(9)	−220(5)	3674(3)
C(11)	4459(8)	1350(5)	2899(3)
C(12)	5029(8)	1732(5)	3443(3)
C(13)	5476(8)	2488(5)	3274(3)
C(14)	5233(8)	2582(4)	2619(3)
C(15)	5621(7)	3274(5)	2252(3)
C(151)	6409(8)	3928(5)	2573(3)
C(152)	7763(9)	3819(5)	2715(3)
C(153)	8484(9)	4438(6)	3008(3)
C(154)	7900(11)	5173(6)	3159(4)
C(155)	6542(11)	5290(5)	3047(4)
C(156)	5803(10)	4669(5)	2746(3)
C(16)	5401(8)	3356(4)	1593(3)
C(17)	5935(9)	4030(4)	1222(3)
C(18)	5604(9)	3856(5)	618(3)
C(19)	4857(8)	3083(4)	615(3)
C(20)	4390(8)	2681(5)	73(3)
C(201)	4648(9)	3054(4)	−554(3)
C(202)	5896(10)	2961(5)	−832(3)
C(203)	6057(10)	3220(6)	−1450(4)
C(204)	5024(10)	3583(5)	−1782(3)
C(205)	3788(10)	3698(5)	−1500(3)
C(206)	3583(9)	3426(5)	−880(3)

by Microchemical Laboratories, University of California, Berkeley. Electronic absorption spectra were recorded with a Hewlett-Packard 8450A spectrophotometer, proton NMR spectra at 300 MHz on a General Electrics QE-300 instrument with shifts referenced to the solvent residue at δ 7.26 for $CHCl_3$.

Syntheses.—The thallium complexes of coproporphyrin I and II (3,8,13,18-tetramethylporphyrin-2,7,12,17-tetrapropionic acid and 3,7,13,17-tetramethylporphyrin-2,8,12,18-tetrapropionic acid) tetramethyl esters[21] (H_2L^1 and H_2L^2) and cyano(2,3,7,8,12,13,17,18-octaethylporphyrinato)thallium(III) [Tl(oep)(CN)][22] were prepared as described previously and gave satisfactory analyical data. 5,10,15,20-tetraphenylporphyrin (H_2tpp) and 5,10,15,20-tetra(4-methoxyphenyl)porphyrin (H_2tmpp) were obtained from Aldrich.

(5,10,15,20-*Tetraphenylporphyrinato*)(*trifluoroacetato*)*thallium*(III), [Tl(tpp)(O_2CCF_3)]. The compound H_2tpp (0.135 mmol) was dissolved in dichloromethane (60 cm^3) and tetrahydrofuran (thf) (30 cm^3). A solution of thallium(III) trifluoroacetate (≈0.5 mmol) in methanol (40 cm^3) was added and the mixture stirred for 2.5 h at room temperature. The reaction mixture was washed with water (3 × 50 cm^3), the organic phase dried over Na_2SO_4 and then evaporated. The residue was recrystallized from CH_2Cl_2–hexane yielding bright

Table 11 Atomic coordinates (× 10^4) for [Tl(tpp)I]

Atom	*x*	*y*	*z*
Tl	1683(1)	1806(1)	1551(1)
I	4192(1)	2433(1)	1782(1)
N(21)	363(6)	1838(3)	2387(2)
N(22)	1701(7)	476(2)	1747(3)
N(23)	1458(6)	1372(2)	575(2)
N(24)	224(6)	2761(3)	1230(1)
C(1)	−245(7)	2534(4)	2598(4)
C(2)	−493(9)	2436(6)	3249(4)
C(3)	−40(9)	1689(5)	3420(4)
C(4)	501(8)	1310(4)	2877(3)
C(5)	1066(8)	528(5)	2856(4)
C(51)	984(6)	41(5)	3431(3)
C(52)	−270(7)	−226(5)	3639(3)
C(53)	−411(8)	−651(6)	4189(3)
C(54)	738(7)	−817(6)	4547(4)
C(55)	2011(7)	−587(6)	4338(3)
C(56)	2120(8)	−161(6)	3787(4)
C(6)	1615(8)	135(5)	2327(3)
C(7)	2054(9)	−693(5)	2302(4)
C(8)	2395(9)	−849(5)	1712(4)
C(9)	2187(8)	−111(5)	1355(4)
C(10)	2357(8)	−24(5)	721(4)
C(101)	2884(6)	−748(5)	371(3)
C(102)	4188(7)	−1037(5)	489(4)
C(103)	4673(10)	−1699(6)	163(4)
C(104)	3894(8)	−2067(6)	−298(4)
C(105)	2594(8)	−1772(5)	−419(4)
C(106)	2101(8)	−1118(5)	−88(3)
C(11)	1988(8)	661(3)	351(4)
C(12)	2113(9)	732(6)	−304(4)
C(13)	1586(9)	1446(6)	−474(4)
C(14)	1218(9)	1884(5)	82(3)
C(15)	624(8)	2646(5)	105(4)
C(151)	389(8)	3042(5)	−512(4)
C(152)	1436(8)	3424(6)	−823(3)
C(153)	1226(8)	3729(6)	−1415(3)
C(154)	−43(7)	3672(6)	−1702(4)
C(155)	−1098(9)	3288(6)	−1398(4)
C(156)	−879(10)	2982(7)	−806(4)
C(16)	140(8)	3051(5)	634(2)
C(17)	−545(9)	3819(6)	637(5)
C(18)	−918(9)	3970(6)	1225(4)
C(19)	−406(8)	3319(4)	1603(3)
C(20)	−622(8)	3204(5)	2241(4)
C(201)	−1395(6)	3865(4)	2563(4)
C(202)	−2732(6)	3735(4)	2738(4)
C(203)	−3493(8)	4336(4)	3021(4)
C(204)	−2896(8)	5083(5)	3140(4)
C(205)	−1547(8)	5220(5)	2986(5)
C(206)	−813(8)	4612(4)	2697(4)

Table 12 Atomic coordinates (× 10^4) for [Tl(tmpp)I]·CH_3OH

Atom	*x*	*y*	*z*
Tl	551(1)	3 324(1)	2 892(1)
I	−756(1)	2 046(1)	2 382(1)
N(21)	1 546(6)	4 312(5)	1 704(4)
N(22)	2 437(5)	2 370(6)	2 634(4)
N(23)	375(4)	3 054(4)	4 348(3)
N(24)	−504(5)	4 963(3)	3 387(2)
C(1)	1 028(8)	5 279(5)	1 382(6)
C(2)	1 740(9)	5 444(8)	450(6)
C(3)	2 682(9)	4 618(8)	196(6)
C(4)	2 580(7)	3 888(7)	981(5)
C(5)	3 432(9)	2 936(8)	1 024(6)
C(51)	4 531(8)	2 619(6)	187(6)
C(52)	5 421(7)	3 287(7)	−219(6)
C(53)	6 471(8)	2 930(6)	−962(6)
C(54)	6 658(5)	1 886(6)	−1 299(5)
C(55)	5 764(7)	1 214(7)	−921(6)
C(56)	4 712(8)	1 596(7)	−186(6)
C(57)	8 222(10)	479(3)	−2 110(8)
C(6)	3 393(7)	2 273(8)	1 799(5)
C(7)	4 358(10)	1 394(9)	1 887(7)
C(8)	3 953(10)	982(8)	2 747(7)
C(9)	2 750(9)	1 589(7)	3 229(6)
C(10)	2 026(9)	1 450(8)	4 163(6)
C(101)	2 504(9)	437(7)	4 610(6)
C(102)	2 463(13)	−600(6)	4 358(9)
C(103)	2 937(14)	−1 536(7)	4 753(9)
C(104)	3 459(9)	−1 443(3)	5 408(6)
C(105)	3 489(10)	−419(5)	5 691(7)
C(106)	3 012(10)	498(7)	5 279(7)
C(107)	4 525(14)	−2 354(11)	6 360(8)
C(11)	951(8)	2 122(5)	4 669(6)
C(12)	229(10)	1 936(9)	5 616(7)
C(13)	−762(10)	2 734(9)	5 847(7)
C(14)	−689(5)	3 462(7)	5 055(5)
C(15)	−1 537(9)	4 370(8)	4 986(7)
C(151)	−2 734(7)	4 602(8)	5 792(5)
C(152)	−2 773(7)	4 875(8)	6 646(5)
C(153)	−3 883(6)	5 069(8)	7 377(5)
C(154)	−4 983(6)	4 968(8)	7 261(4)
C(155)	−4 958(7)	4 657(7)	6 422(4)
C(156)	−3 838(6)	4 471(8)	5 698(5)
C(157)	−7 183(8)	5 133(12)	7 907(8)
C(16)	−1 439(6)	5 099(8)	4 231(3)
C(17)	−2 259(10)	6 100(9)	4 222(7)
C(18)	−1 824(10)	6 564(8)	3 372(7)
C(19)	−748(9)	5 850(5)	2 848(6)
C(20)	−53(9)	5 993(8)	1 916(6)
C(201)	−482(9)	7 017(6)	1 457(6)
C(202)	−465(10)	8 049(5)	1 735(7)
C(203)	−952(9)	9 004(7)	1 370(6)
C(204)	−1 421(9)	8 924(6)	682(6)
C(205)	−1 381(10)	7 902(6)	358(6)
C(206)	−905(9)	6 957(7)	741(6)
C(207)	−1 993(13)	10 842(7)	592(8)
O(1)	7 731(6)	1 602(4)	−2 028(4)
O(2)	3 950(9)	−2 417(4)	5 721(6)
O(3)	−6 050(6)	5 199(7)	8 006(5)
O(4)	−1 886(9)	9 805(5)	245(6)

red crystals (0.125 mmol, 93%), m.p. > 300 °C (Found: C, 59.70; H, 3.20; N, 6.20. $C_{46}H_{28}F_3N_4O_2Tl$ requires C, 59.40; H, 3.05; N, 6.00%); $\lambda_{max}(CH_2Cl_2)$/nm (10^{-3} ε/dm^3 mol^{-1} cm^{-1}) 432 (447.1), 566 (30.8) and 606 (20.6); δ_H(300 MHz, $CDCl_3$) 9.09 [8 H, d, β-H, $J(^1H-^{203,205}Tl)$ 73 Hz], 8.26 (8 H, m, *o*-H) and 7.82 (12 H, m, *m*,*p*-H).

[5,10,15,20-*Tetra*(4-*methoxyphenyl*)*porphyrinato*](*trifluoroacetato*)*thallium*(III), [Tl(tmpp)(O_2CCF_3)]. This was prepared in the same manner as red crystals, yield 91%, m.p. 285–287 °C (Found: C, 57.40; H, 3.70; N, 5.55. $C_{50}H_{36}F_3N_4O_6Tl$ requires C, 57.20; H, 3.45; N, 5.35%); $\lambda_{max}(CH_2Cl_2)$/nm (10^{-3} ε/dm^3 mol^{-1} cm^{-1}) 438 (475.5), 570 (16.5) and 612 (16.1); δ_H(300 MHz, $CDCl_3$) 9.10 (8 H, d, β-H, $J(^1H-^{203,205}Tl)$ 67 Hz], 8.15 (8 H, m, *o*-H), 7.27 (8 H, m, *m*-H) and 4.18 (12 H, s, *p*-OCH_3).

Chloro[5,10,15,20-*tetra*(4-*methoxyphenyl*)*porphyrinato*]*thallium*(III), [Tl(tmpp)Cl]. The complex [Tl(tmpp)(O_2CCF_3)] (0.250 mmol) was dissolved in dichloromethane (70 cm^3) and tetrahydrofuran (30 cm^3). Potassium chloride (5 mmol) was added and the mixture was stirred for 4 h at room temperature. It was washed with water (3 × 50 cm^3), the organic phase dried

Table 13 Atomic coordinates (× 10^4) for [Tl(tmpp)(CN)]

Atom	*x*	*y*	*z*
Tl	1 846(1)	3 554(1)	2 736(1)
C(1a)	3 150(6)	2 334(5)	2 797(5)
N(1a)	3 834(6)	1 730(6)	2 884(5)
N(21)	2 584(4)	5 220(4)	3 472(3)
N(22)	1 842(4)	4 435(4)	1 467(3)
N(23)	200(4)	2 684(4)	1 973(3)
N(24)	899(4)	3 502(4)	3 973(3)
C(1)	2 704(5)	5 511(5)	4 413(4)
C(2)	3 384(5)	6 602(5)	4 637(4)
C(3)	3 658(5)	6 934(5)	3 815(4)
C(4)	3 161(5)	6 063(5)	3 085(4)
C(5)	3 226(5)	6 092(5)	2 132(4)
C(51)	3 970(5)	7 066(5)	1 873(4)
C(52)	5 177(5)	7 137(5)	2 027(4)
C(53)	5 856(5)	8 049(5)	1 803(4)
C(54)	5 322(5)	8 944(5)	1 446(4)
C(55)	4 117(6)	8 895(5)	1 305(5)
C(56)	3 446(6)	7 950(5)	1 500(4)
C(57)	5 543(6)	10 843(5)	1 137(5)
C(6)	2 616(5)	5 342(5)	1 392(4)
C(7)	2 691(5)	5 392(5)	421(4)
C(8)	1 980(5)	4 535(5)	−69(4)
C(9)	1 425(5)	3 923(5)	583(4)
C(10)	548(5)	3 012(5)	362(4)
C(101)	175(5)	2 591(5)	−646(4)
C(102)	−193(5)	3 304(5)	−1 291(4)
C(103)	−617(5)	2 891(5)	−2 209(4)
C(104)	−753(5)	1 741(5)	−2 491(4)
C(105)	−342(6)	1 010(5)	−1 872(4)
C(106)	118(6)	1 438(5)	−972(4)
C(107)	−2 047(6)	362(6)	−3 494(5)
C(11)	−51(5)	2 478(5)	1 008(4)
C(12)	−1 035(5)	1 634(5)	781(4)
C(13)	−1 343(5)	1 333(5)	1 602(4)
C(14)	−574(5)	1 992(5)	2 347(4)
C(15)	−630(5)	1 958(4)	3 299(4)
C(151)	−1 508(5)	1 090(5)	3 553(4)
C(152)	−2 691(5)	1 228(5)	3 473(4)
C(153)	−3 479(6)	433(5)	3 733(4)
C(154)	−3 093(5)	−532(5)	4 057(4)
C(155)	−1 928(6)	−701(5)	4 114(4)
C(156)	−1 142(5)	111(5)	3 873(4)
C(157)	−3 520(6)	−2 255(6)	4 655(5)
C(16)	47(5)	2 668(5)	4 048(4)
C(17)	−80(5)	2 655(5)	5 014(4)
C(18)	714(5)	3 457(5)	5 507(4)
C(19)	1 337(5)	4 006(5)	4 865(4)
C(20)	2 211(5)	4 920(5)	5 077(4)
C(201)	2 666(5)	5 286(5)	6 078(4)
C(202)	1 939(5)	5 603(5)	6 743(4)
C(203)	2 389(5)	5 974(5)	7 664(4)
C(204)	3 590(5)	6 037(5)	7 941(4)
C(205)	4 315(5)	5 716(5)	7 291(4)
C(206)	3 856(5)	5 342(5)	6 371(4)
C(207)	5 167(6)	6 468(6)	9 177(4)
O(1)	6 041(4)	9 812(3)	1 250(3)
O(2)	−1 275(4)	1 384(4)	−3 375(3)
O(3)	−3 918(4)	−1 266(4)	4 322(3)
O(4)	3 942(4)	6 444(3)	8 851(3)

Table 14 Atomic coordinates (× 10^4) for [Tl(oep)(CN)]

Atom	*x*	*y*	*z*
Tl	1071(1)	2675(1)	2812(1)
C(1a)	2463(7)	2673(7)	4095(5)
N(1a)	3199(7)	2708(8)	4746(5)
N(21)	340(5)	629(3)	1665(3)
N(22)	−1013(3)	2339(4)	2909(4)
N(23)	856(3)	4809(3)	3108(3)
N(24)	2204(5)	3107(2)	1856(3)
C(1)	1054(6)	32(2)	1060(4)
C(2)	487(6)	−1429(6)	626(4)
C(21)	965(6)	−2431(6)	−89(4)
C(22)	2128(6)	−2931(7)	378(5)
C(3)	−536(6)	−1684(5)	1009(5)
C(31)	−1380(6)	−3041(5)	829(5)
C(32)	−830(7)	−3654(7)	1558(5)
C(4)	−633(6)	−382(6)	1656(5)
C(5)	−1565(7)	−160(7)	2170(5)
C(6)	−1768(6)	1080(5)	2748(5)
C(7)	−2796(6)	1257(6)	3232(5)
C(71)	−3794(5)	130(6)	3247(4)
C(72)	−4948(7)	−536(8)	2332(5)
C(8)	−2655(6)	2643(6)	3691(4)
C(81)	−3504(6)	3362(6)	4255(4)
C(82)	−4525(7)	3876(8)	3667(6)
C(9)	−1503(6)	3310(5)	3496(4)
C(10)	−984(6)	4715(7)	3847(5)
C(11)	110(6)	5415(6)	3683(4)
C(12)	643(7)	6879(6)	4098(4)
C(121)	79(6)	7892(6)	4739(4)
C(122)	−1080(6)	8319(7)	4201(5)
C(13)	1710(6)	7129(5)	3754(5)
C(131)	2599(6)	8471(5)	3954(5)
C(132)	2139(8)	9089(8)	3211(5)
C(14)	1843(5)	5827(5)	3138(5)
C(15)	2765(6)	5605(6)	2612(5)
C(16)	2928(6)	4375(3)	2006(5)
C(17)	3865(6)	4195(6)	1434(5)
C(171)	4768(6)	5352(6)	1372(5)
C(172)	6005(6)	6052(7)	2228(5)
C(18)	3707(6)	2825(7)	975(4)
C(181)	4482(6)	2143(7)	329(4)
C(182)	5686(7)	1759(8)	854(6)
C(19)	2641(6)	2137(5)	1228(3)
C(20)	2120(7)	728(7)	877(5)

over Na_2SO_4 and evaporated. The residue was recrystallized from CH_2Cl_2–hexane yielding bright purple crystals (0.223 mmol, 89%), m.p. > 300 °C (Found: C, 59.45; H, 3.70; N, 5.80. $C_{48}H_{36}ClN_4O_4Tl$ requires C, 59.25; H, 3.75; N, 5.75%); $\lambda_{max}(CH_2Cl_2)$/nm (10^{-3} ε/dm^3 mol^{-1} cm^{-1}) 438 (424.8), 572 (16.2) and 614 (16.5); δ_H(300 MHz, $CDCl_3$) 9.09 [8 H, d, β-H, $J(^1H-^{203,205}Tl)$ 65 Hz], 8.15 (8 H, m, *o*-H), 7.32 (8 H, m, *m*-H) and 4.13 (12 H, s, *p*-OCH_3).

Bromo(5,10,15,20-*tetraphenylporphyrinato*)*thallium*(III), [Tl(tpp)Br]. This was prepared similarly to the above using KBr in thf. Bright purple crystals, yield 94%, m.p. > 300 °C (Found: C, 58.90; H, 3.05; N, 6.20. $C_{44}H_{28}BrN_4Tl$ requires C, 58.90; H, 3.15; N, 6.25%); $\lambda_{max}(CHCl_3)$/nm (10^{-3} ε/dm^3 mol^{-1} cm^{-1}) 434 (395.1), 566 (13.6) and 606 (7.8); δ_H(300 MHz, $CDCl_3$) 9.05 [8 H, d, β-H, $J(^1H-^{203,205}Tl)$ 60 Hz], 8.25 (8 H, m, *o*-H) and 7.79 (12 H, m, *m*,*p*-H).

Iodo(5,10,15,20-*tetraphenylporphyrinato*)*thallium*(III), [Tl(tpp)I]. This was prepared as above using KI in methanol. Bright purple crystals, yield 85%, m.p. > 300 °C (Found: C, 56.05; H, 2.95; N, 6.00. $C_{44}H_{28}IN_4Tl$ requires C, 56.00; H, 3.00; N, 5.95%); $\lambda_{max}(CH_2Cl_2)$/nm (10^{-3} ε/dm^3 mol^{-1} cm^{-1}) 438 (475), 570 (16.5) and 610 (10.2); δ_H(300 MHz, $CDCl_3$) 8.91 [8 H, d, β-H, $J(^1H-^{203,205}Tl)$ 52 Hz], 8.22 (8 H, m, *o*-H) and 7.78 (12 H, m, *m*,*p*-H).

Iodo[5,10,15,20-*tetra*(4-*methoxyphenyl*)*porphyrinato*]-*thallium*(III), [Tl(tmpp)I]. This was prepared as described above

Table 15 Atomic coordinates (× 10^4) for [Tl(tpp)(SCN)]

Atom	*x*	*y*	*z*
Tl	4 687(1)	6 397(1)	7 266(1)
S(1a)	6 044(2)	7 332(1)	7 743(1)
C(1a)	5 189(7)	8 687(6)	7 418(5)
N(1a)	4 651(7)	9 607(5)	7 209(5)
N(21)	3 682(4)	5 478(3)	8 533(3)
N(22)	2 588(3)	7 687(3)	7 491(3)
N(23)	4 876(3)	6 800(2)	5 699(2)
N(24)	5 985(4)	4 650(2)	6 753(2)
C(1)	4 311(6)	4 393(4)	8 878(4)
C(2)	3 484(7)	4 252(6)	9 857(5)
C(3)	2 396(7)	5 226(5)	10 095(5)
C(4)	2 489(5)	6 011(5)	9 254(4)
C(5)	1 493(6)	7 104(5)	9 183(4)
C(51)	206(5)	7 439(4)	10 048(4)
C(52)	−680(5)	6 830(5)	10 281(4)
C(53)	−1 862(6)	7 107(5)	11 077(4)
C(54)	−2 195(6)	8 023(5)	11 637(4)
C(55)	−1 318(5)	8 642(5)	11 403(4)
C(56)	−125(6)	8 348(5)	10 617(4)
C(6)	1 551(5)	7 865(5)	8 369(3)
C(7)	456(6)	8 928(5)	8 258(5)
C(8)	863(6)	9 363(5)	7 341(5)
C(9)	2 192(6)	8 584(4)	6 851(4)
C(10)	2 966(6)	8 678(5)	5 859(4)
C(101)	2 430(6)	9 783(4)	5 318(4)
C(102)	2 669(8)	10 732(4)	5 469(5)
C(103)	2 226(8)	11 765(5)	4 969(5)
C(104)	1 542(7)	11 852(5)	4 301(5)
C(105)	1 312(8)	10 907(4)	4 131(6)
C(106)	1 759(8)	9 880(5)	4 638(5)
C(11)	4 178(6)	7 845(2)	5 327(4)
C(12)	4 880(7)	7 947(6)	4 303(4)
C(13)	5 993(7)	6 971(5)	4 078(4)
C(14)	6 019(4)	6 252(5)	4 953(3)
C(15)	7 042(6)	5 180(5)	5 039(4)
C(151)	8 250(5)	4 820(4)	4 145(4)
C(152)	9 281(6)	5 286(6)	3 891(5)
C(153)	10 388(7)	4 985(6)	3 049(5)
C(154)	10 483(6)	4 203(5)	2 439(4)
C(155)	9 478(6)	3 709(6)	2 703(4)
C(156)	8 380(6)	4 006(6)	3 550(4)
C(16)	7 010(5)	4 434(5)	5 868(3)
C(17)	8 013(7)	3 292(5)	5 917(5)
C(18)	7 561(7)	2 850(5)	6 829(5)
C(19)	6 302(6)	3 690(3)	7 354(4)
C(20)	5 516(6)	3 555(5)	8 328(5)
C(201)	5 954(6)	2 378(4)	8 803(4)
C(202)	5 917(7)	1 461(4)	8 416(4)
C(203)	6 294(7)	373(4)	8 851(4)
C(204)	6 727(7)	188(5)	9 673(4)
C(205)	6 760(7)	1 101(4)	10 068(4)
C(206)	6 391(6)	2 184(4)	9 625(4)

Table 16 Atomic coordinates (× 10^4) for [Tl(tmpp)(SCN)]·2CH$_2$Cl$_2$

Atom	*x*	*y*	*z*
Tl	3 727(1)	3 340(1)	1 478(1)
S(1a)	2 572(1)	3 720(1)	2 849(1)
C(1a)	1 811(5)	2 473(5)	2 342(5)
N(1a)	1 273(6)	1 640(5)	2 019(5)
N(21)	2 639(3)	2 021(2)	92(2)
N(22)	3 483(3)	4 269(2)	708(2)
N(23)	5 486(2)	4 350(2)	2 077(3)
N(24)	4 637(2)	2 108(2)	1 472(2)
C(1)	2 431(4)	988(3)	−112(3)
C(2)	1 520(4)	408(4)	−987(4)
C(3)	1 157(4)	1 093(4)	−1 258(4)
C(4)	1 855(3)	2 116(4)	−577(3)
C(5)	1 779(4)	3 044(4)	−610(3)
C(51)	827(3)	2 974(3)	−1 391(3)
C(52)	904(4)	2 464(4)	−2 384(3)
C(53)	45(3)	2 416(4)	−3 107(3)
C(54)	−910(4)	2 867(4)	−2 848(3)
C(55)	−1 001(4)	3 361(4)	−1 859(3)
C(56)	−134(3)	3 417(4)	−1 136(3)
C(57)	−2 676(5)	3 253(5)	−3 372(5)
C(6)	2 531(3)	4 042(4)	−17(3)
C(7)	2 462(4)	4 962(4)	−110(4)
C(8)	3 350(4)	5 737(4)	569(4)
C(9)	4 024(4)	5 302(3)	1 073(3)
C(10)	5 086(4)	5 810(4)	1 764(3)
C(101)	5 531(4)	6 955(3)	2 145(3)
C(102)	5 696(4)	7 396(3)	1 536(3)
C(103)	6 136(4)	8 464(3)	1 936(3)
C(104)	6 436(4)	9 114(3)	2 957(3)
C(105)	6 268(5)	8 692(3)	3 580(3)
C(106)	5 809(4)	7 625(3)	3 163(3)
C(107)	7 253(7)	10 832(5)	4 310(5)
C(11)	5 790(4)	5 323(2)	2 149(3)
C(12)	6 995(4)	5 740(4)	2 662(4)
C(13)	7 368(4)	5 041(4)	2 908(4)
C(14)	6 419(3)	4 172(4)	2 557(3)
C(15)	6 454(4)	3 270(4)	2 665(3)
C(151)	7 517(4)	3 306(3)	3 325(3)
C(152)	7 820(4)	4 049(4)	4 326(3)
C(153)	8 799(4)	4 077(4)	4 938(3)
C(154)	9 504(4)	3 362(3)	4 538(3)
C(155)	9 233(4)	2 624(4)	3 537(3)
C(156)	8 241(3)	2 601(3)	2 941(3)
C(157)	11 210(5)	2 745(6)	4 795(5)
C(16)	5 612(3)	2 327(4)	2 174(3)
C(17)	5 643(4)	1 417(4)	2 298(4)
C(18)	4 699(4)	676(4)	1 690(3)
C(19)	4 063(3)	1 097(2)	1 160(3)
C(20)	3 048(4)	553(4)	404(3)
C(201)	2 571(3)	−564(3)	111(3)
C(202)	3 268(4)	−1 307(3)	−134(3)
C(203)	2 799(3)	−2 357(3)	−468(3)
C(204)	1 607(3)	−2 675(3)	−596(4)
C(205)	903(4)	−1 939(3)	−321(4)
C(206)	1 393(3)	−886(3)	41(4)
C(207)	74(5)	−4 138(5)	−1 656(5)
O(1)	−1 703(3)	2 785(3)	−3 611(3)
O(2)	6 893(3)	10 144(3)	3 272(3)
O(3)	10 450(3)	3 450(3)	5 191(3)
O(4)	1 197(3)	−3 740(3)	−1 022(3)

using KI in methanol. Bright purple crystals, yield 87%, m.p. > 300 °C (Found: C, 54.00: H, 3.40; N, 5.20. $C_{48}H_{36}IN_4O_4Tl$ requires C, 54.20; H, 3.40; N, 5.25%); $\lambda_{max}(CH_2Cl_2)$/nm (10^{-3} ε/dm^3 mol^{-1} cm^{-1}) 442 (435), 578 (14.9) and 620 (15.4); δ_H(300 MHz, CDCl$_3$) 9.03 [8 H, d, β-H, $J(^1H-^{203,205}Tl)$ 54 Hz], 8.14 (8 H, m, *o*-H), 7.29 (8 H, m, *m*-H) and 4.11 (12 H, s, *p*-OCH$_3$).

Cyano(5,10,15,20-*tetraphenylporphyrinato*)*thallium*(III), [Tl(tpp)(CN)]. This was prepared as above using KCN in methanol. Bright purple crystals, yield 81.5%, m.p. > 300 °C (Found: C, 63.90; H, 3.30; N, 8.30. $C_{45}H_{28}N_5Tl$ requires C, 64.10; H, 3.35; N, 8.30%); $\lambda_{max}(CH_2Cl_2)$/nm (10^{-3} ε/dm^3 mol^{-1} cm^{-1}) 434 (448), 568 (14.2) and 608 (9.1); δ_H(300 MHz, CDCl$_3$) 8.73 [8 H, d, β-H, $J(^1H-^{203,205}Tl)$ 58 Hz], 8.18 (8 H, m, *o*-H) and 7.75 (12 H, m, *m*,*p*-H).

Cyano[5,10,15,20-*tetra*(4-*methoxyphenyl*)*porphyrinato*]-*thallium*(III), [Tl(tmpp)(CN)]. This was prepared above using KCN in methanol. Bright purple crystals, yield 92%, m.p. > 300 °C (Found: C, 60.95; H, 3.80; N, 7.30. $C_{49}H_{36}N_5O_4Tl$

Table 17 Atomic coordinates (× 10^4) for [Tl(tpp)(N_3)]

Atom	*x*	*y*	*z*	Atom	*x*	*y*	*z*
Tl	268(1)	3633(1)	2704(1)	C(103)	−1318(8)	9602(5)	1144(5)
N(1)	−823(7)	2710(6)	2293(5)	C(104)	−1695(8)	9797(6)	277(5)
N(2)	−362(8)	1699(7)	2487(6)	C(105)	−1720(8)	8897(5)	−146(5)
N(3)	45(9)	716(7)	2648(6)	C(106)	−1356(8)	7809(5)	280(5)
N(21)	82(6)	3239(4)	4306(3)	C(11)	666(7)	5597(3)	1067(5)
N(22)	−1056(6)	5386(3)	3233(3)	C(12)	1528(8)	5745(7)	66(6)
N(23)	1316(3)	4523(2)	1411(3)	C(13)	2651(8)	4754(7)	−155(5)
N(24)	2416(4)	2330(4)	2480(2)	C(14)	2544(4)	3995(6)	691(4)
C(1)	802(7)	2207(4)	4680(5)	C(15)	3537(9)	2902(7)	768(5)
C(2)	89(8)	2147(7)	5738(6)	C(151)	4855(7)	2545(5)	−96(5)
C(3)	−1030(9)	3125(5)	5964(6)	C(152)	5775(7)	3125(6)	−314(5)
C(4)	−1062(6)	3811(6)	5064(5)	C(153)	6992(7)	2818(6)	−1111(5)
C(5)	−2105(8)	4870(7)	4978(6)	C(154)	7298(7)	1942(6)	−1716(5)
C(51)	−3363(7)	5247(6)	5877(5)	C(155)	6391(6)	1351(6)	−1495(5)
C(52)	−4365(7)	4744(7)	6123(5)	C(156)	5170(7)	1663(6)	−700(5)
C(53)	−5527(8)	5097(7)	6953(6)	C(16)	3484(6)	2146(6)	1598(3)
C(54)	−5707(7)	5934(6)	7556(5)	C(17)	4585(8)	1070(6)	1695(5)
C(55)	−4696(7)	6428(7)	7310(5)	C(18)	4161(8)	636(7)	2630(6)
C(56)	−3539(8)	6090(6)	6473(5)	C(19)	2789(8)	1439(4)	3133(5)
C(6)	−2082(7)	5602(6)	4135(4)	C(20)	2022(8)	1351(6)	4144(6)
C(7)	−3117(8)	6735(6)	4068(6)	C(201)	2514(7)	247(5)	4675(5)
C(8)	−2658(9)	7166(7)	3140(6)	C(202)	3209(9)	104(5)	5373(6)
C(9)	−1349(8)	6315(5)	2601(5)	C(203)	3623(9)	−930(5)	5881(6)
C(10)	−560(8)	6449(7)	1621(5)	C(204)	3308(9)	−1828(6)	5712(6)
C(101)	−985(8)	7624(6)	1150(4)	C(205)	2600(10)	−1685(6)	5023(6)
C(102)	−957(8)	8518(5)	1578(5)	C(206)	2209(9)	−657(5)	4506(6)

Table 18 Atomic coordinates (× 10^4) for [Tl(tmpp)(N_3)]·CH_2Cl_2

Atom	*x*	*y*	*z*	Atom	*x*	*y*	*z*
Tl	590(1)	2 513(1)	3 961(1)	C(106)	−2 377(5)	1 842(5)	7 153(4)
N(1)	−806(5)	2 557(4)	2 962(3)	C(107)	−2 254(7)	1 135(6)	10 438(4)
N(2)	−1 584(5)	3 441(5)	2 582(4)	C(11)	−906(5)	3 144(4)	5 597(3)
N(3)	−2 352(7)	4 249(6)	2 205(5)	C(12)	−1 820(5)	4 043(5)	5 753(4)
N(21)	2 539(3)	1 655(3)	3 719(3)	C(13)	−1 925(5)	4 918(5)	4 991(4)
N(22)	1 059(4)	1 195(3)	5 335(2)	C(14)	−1 070(5)	4 603(3)	4 346(4)
N(23)	−452(4)	3 512(3)	4 739(2)	C(15)	−833(5)	5 277(4)	3 477(4)
N(24)	1 009(4)	3 960(2)	3 106(3)	C(151)	−1 734(5)	6 416(4)	3 082(3)
C(1)	3 126(5)	2 048(4)	2 933(3)	C(152)	−1 949(5)	7 103(3)	3 563(3)
C(2)	4 075(6)	1 162(5)	2 791(4)	C(153)	−2 748(5)	8 162(3)	3 164(3)
C(3)	4 029(6)	259(5)	3 469(4)	C(154)	−3 381(5)	8 537(3)	2 281(3)
C(4)	3 081(5)	555(3)	4 067(4)	C(155)	−3 206(5)	7 853(3)	1 801(4)
C(5)	2 791(5)	−143(4)	4 895(4)	C(156)	−2 393(5)	6 799(4)	2 207(3)
C(51)	3 493(4)	−1 311(4)	5 185(4)	C(157)	−4 748(7)	10 020(5)	1 025(3)
C(52)	4 818(4)	−1 752(3)	5 349(4)	C(16)	171(5)	4 983(3)	2 933(4)
C(53)	5 453(5)	−2 848(3)	5 644(4)	C(17)	528(6)	5 715(5)	2 118(4)
C(54)	4 751(4)	−3 525(3)	5 796(4)	C(18)	1 569(6)	5 112(5)	1 837(4)
C(55)	3 426(4)	−3 105(3)	5 625(4)	C(19)	1 861(5)	4 016(5)	2 432(3)
C(56)	2 817(5)	−2 005(3)	5 323(4)	C(20)	2 845(5)	3 129(5)	2 354(4)
C(57)	4 771(6)	−5 310(4)	6 265(5)	C(201)	3 675(4)	3 361(4)	1 574(3)
C(6)	1 895(5)	175(3)	5 502(4)	C(202)	3 198(5)	3 729(5)	646(3)
C(7)	1 743(6)	−493(5)	6 414(4)	C(203)	3 974(4)	3 897(5)	−82(3)
C(8)	823(6)	120(5)	6 781(4)	C(204)	5 264(4)	3 684(4)	122(3)
C(9)	380(5)	1 187(5)	6 103(3)	C(205)	5 749(5)	3 344(5)	1 044(3)
C(10)	−531(5)	2 077(5)	6 215(4)	C(206)	4 962(4)	3 170(5)	1 764(3)
C(101)	−1 140(4)	1 868(5)	7 121(3)	C(207)	5 658(6)	4 063(6)	−1 473(3)
C(102)	−483(5)	1 682(5)	7 948(3)	O(1)	5 456(4)	−4 593(3)	6 122(3)
C(103)	−1 034(4)	1 487(5)	8 791(3)	O(2)	−2 902(5)	1 271(4)	9 600(3)
C(104)	−2 272(4)	1 466(5)	8 810(3)	O(3)	−4 141(4)	9 590(3)	1 949(3)
C(105)	−2 943(6)	1 654(6)	7 989(3)	O(4)	6 114(4)	3 804(4)	−537(3)

requires C, 61.10; H, 3.75; N, 7.25%); $\lambda_{max}(CH_2Cl_2)$/nm (10^{-3} ε/dm^3 mol^{-1} cm^{-1}) 438 (402.7), 572 (11.2) and 616 (13); δ_H(300 MHz, $CDCl_3$) 9.08 [8 H, d, β-H, $J(^1H-^{203,205}Tl)$ 62 Hz], 8.15 (8 H, m, *o*-H), 7.41–7.27 (8 H, m, *m*-H) and 4.12 (12 H, s, *p*-OCH_3).

(5,10,15,20-*Tetraphenylporphyrinato*)*thiocyanatothallium*(III) [Tl(tpp)(SCN)]. This was prepared as above using KSCN in methanol. Bright purple crystals, yield 76%, m.p. > 300 °C (Found: C, 62.00; H, 3.10; N, 7.85. $C_{45}H_{28}N_5STl$ requires C, 61.75; H, 3.25; N, 8.00%); $\lambda_{max}(CH_2Cl_2)$/nm (10^{-3} ε/dm^3 mol^{-1} cm^{-1}) 436 (389.4), 568 (40.9) and 608 (35.4); δ_H(300 MHz, $CDCl_3$) 9.06 [8 H, d, β-H, $J(^1H-^{203,205}Tl)$ 61 Hz], 8.23 (8 H, m, *o*-H) and 7.79 (12 H, m, *m,p*-H).

[5,10,15,20-*Tetra*(4-*methoxyphenyl*)*porphyrinato*]*thiocyanatothallium*(III), [Tl(tmpp)(SCN)]. This was prepared as described above using KSCN in methanol. Bright purple crystals, yield 86%, m.p. 280–282 °C (Found: C, 58.95; H, 3.60; N, 7.30. $C_{49}H_{36}N_5O_4STl$ requires C, 59.15; H, 3.65; N, 7.05%); $\lambda_{max}(CH_2Cl_2)$/nm (10^{-3} ε/dm^3 mol^{-1} cm^{-1}) 440 (297.5), 572

(19.6) and 616 (21.5); δ_H(300 MHz, $CDCl_3$) 9.11 [8 H, d, β-H, $J(^1H-^{203,205}Tl)$ 60 Hz], 8.15 (8 H, m, *o*-H), 7.29 (8 H, m, *m*-H) and 4.11 (12 H, s, *p*-OCH_3).

Azido(5,10,15,20-*tetraphenylporphyrinato*)*thallium*(III), [Tl(tpp)(N_3)]. This was described as above using KN_3 in methanol. Bright purple crystals, yield 90%, m.p. >270 °C (Found: C, 61.50; H, 3.35; N, 11.35. $C_{44}H_{28}N_7Tl$ requires C, 61.50; H, 3.30; N, 11.40%); $\lambda_{max}(CH_2Cl_2)$/nm (10^{-3} ε/dm³ mol⁻¹ cm⁻¹) 432 (335.1), 564 (20.8) and 606 (11.6); δ_H(300 MHz, $CDCl_3$) 9.05 [8 H, d, β-H, $J(^1H-^{203,205}Tl)$ 62 Hz], 8.22 (8 H, m, *o*-H) and 7.76 (12 H, m, *m*,*p*-H).

Azido[5,10,15,20-*tetra*(4-*methoxyphenyl*)*porphyrinato*]*thallium*(III), [Tl(tmpp)(N_3)]. This was prepared as described above using KN_3 in methanol. Bright purple crystals, yield 80%, m.p. >270 °C (Found: C, 59.00; H, 3.95; N, 10.20. $C_{48}H_{36}N_7O_4Tl$ requires C, 58.90; H, 3.70; N, 10.00%); $\lambda_{max}(CH_2Cl_2)$/nm (10^{-3} ε/dm³ mol⁻¹ cm⁻¹) 438 (398.4), 570 (7.7) and 614 (8); δ_H(300 MHz, $CDCl_3$) 9.09 [8 H, d, β-H, $J(^1H-^{203,205}Tl)$ 58 Hz], 8.16 (8 H, m, *o*-H), 7.27 (8 H, m, *m*-H) and 4.11 (12 H, s, *p*-OCH_3).

Crystallography.—Crystals were grown by slow diffusion of methanol or hexane into a concentrated solution of the porphyrin complex in methylene chloride. They were immersed in hydrocarbon oil, a single crystal selected, mounted on a glass fibre and placed in the low-temperature nitrogen stream of the diffractometer.[53] For most data collections either a Siemens R3m/V equipped with a locally modified Enraf-Nonius LT device or a Syntex P2$_1$ automatic diffractometer equipped with locally modified Siemens LT device was used, with graphite-monochromated Mo-Kα radiation (λ = 0.7107 Å). Cell parameters were determined from 20–25 automatically centred reflections in the range 20 < 2θ < 25°. For the structure determination of [TlL^1(Cl)] a Siemens P4 instrument equipped with a rotating-anode system operating at 50 kV and 300 mA was employed, with Cu-Kα radiation (λ = 1.5418 Å). Cell parameters were determined from 29 automatically centred reflections in the range 40 < 2θ < 60°. During all data collections two standard reflections were measured every 198 and showed in all cases only statistical variation of the intensities (< 2%). The intensities were corrected for Lorentz and polarization effects. In all structure refinements an absorption correction was applied using the program XABS,[54] while extinction effects were disregarded. All structures were solved *via* Patterson synthesis, followed by structure expansion using the SHELXTL PLUS program system.[55] Missing atoms and/or solvent molecules were located in subsequent Fourier difference maps. Refinements were carried out by full-matrix least squares on $|F|$ using the same program system. Hydrogen atoms were included at calculated positions using a riding model with C–H 0.96 Å. Calculations were carried out on a Vax station 3200. All non-hydrogen atoms were refined with anisotropic thermal parameters.

Additional material available from the Cambridge Crystallographic Data Centre comprises H-atom coordinates, thermal parameters and remaining bond lengths and angles.

Acknowledgements

We thank Dr. Marilyn M. Olmstead for collecting the data on [TlL^1(Cl)]. This work was supported by grants from the Deutsche Forschungsgemeinschaft (Se543/1-1), the National Institutes of Health (HL-22252) and the National Science Foundation (CHE-93-05577).

References

1 W. R. Scheidt and Y. J. Lee, *Struct. Bonding* (*Berlin*), 1987, **64**, 1.
2 M. O. Senge, *J. Photochem. Photobiol. B:Biol.*, 1992, **16**, 3.
3 K. M. Barkigia, L. Chantranupong, K. M. Smith and J. Fajer, *J. Am. Chem. Soc.*, 1988, **110**, 7566.
4 R. Guilard, A. Zrineh, A. Tabard, A. Endo, B. Han, C. Lecomte, M. Souhassou, A. Habbou, M. Ferhat and K. M. Kadish, *Inorg. Chem.*, 1990, **29**, 4476.
5 A. Boukhris, C. Lecomte, A. Coutsolelos and R. Guilard, *J. Organomet. Chem.*, 1986, **303**, 151.
6 A. Coutsolelos, R. Guilard, A. Boukhris and C. Lecomte, *J. Chem. Soc., Dalton Trans.*, 1986, 1779.
7 A. Coutsolelos, R. Guilard, D. Bayeul and C. Lecomte, *Polyhedron*, 1986, **5**, 1157.
8 R. G. Ball, K. M. Lee, A. G. Marshall and J. Trotter, *Inorg. Chem.*, 1980, **19**, 1463.
9 (*a*) R. Guilard, S. S. Gerges, A. Tabard, P. Richard, M. A. El Borai and C. Lecomte, *J. Am. Chem. Soc.*, 1987, **109**, 7228; (*b*) R. Guilard, N. Jagerovic, A. Tabard, P. Richard, L. Courthaudon, A. Louati, C. Lecomte and K. M. Kadish, *Inorg. Chem.*, 1991, **30**, 16.
10 (*a*) R. Guilard, P. Mitaine, C. Lecomte, A. Boukhris, C. Swistak, A. Tabard, D. Lacombe, J.-L. Cornillon and K. M. Kadish, *Inorg. Chem.*, 1987, **26**, 2467; (*b*) C. Lecomte, A. Habbou, P. Mitaine, P. Richard and R. Guilard, *Acta Crystallogr., Sect. C*, 1989, **45**, 1226.
11 C. Lecomte, J. Protas, P. Cocolios and R. Guilard, *Acta Crystallogr., Sect. B*, 1980, **36**, 2769.
12 D. L. Cullen, E. F. Meyer, jun., and K. M. Smith, *Inorg. Chem.*, 1977, **16**, 1179.
13 K. Henrick, R. W. Matthews and P. A. Tasker, *Inorg. Chem.*, 1977, **16**, 3293.
14 F. Brady, K. Henrick and R. W. Matthews, *J. Organomet. Chem.*, 1981, **210**, 281.
15 R. Guilard, A. Zrineh, M. Ferhat, A. Tabard, P. Mitaine, C. Swistak, P. Richard, C. Lecomte and K. M. Kadish, *Inorg. Chem.*, 1988, **27**, 697.
16 P. Richard, A. Zrineh, R. Guilard, A. Habbou and C. Lecomte, *Acta Crystallogr., Sect. C*, 1989, **45**, 1224.
17 M. O. Senge and K. M. Smith, *Z. Naturforsch., Teil B*, 1992, **47**, 837.
18 (*a*) S.-C. Suen, W.-B. Lee, F. E. Hong, T.-T. Jong and J.-H. Chen, *Polyhedron*, 1992, **11**, 3025; (*b*) J. C. Chen, H. S. Jang, J. H. Chen and L. P. Hwang, *Polyhedron*, 1991, **10**, 2069.
19 A. G. Coutsolelos, M. Orfanopoulos and D. L. Ward, *Polyhedron*, 1991, **10**, 885.
20 A. G. Coutsolelos, A. Tsapara, D. Daphnomili and D. L. Ward, *J. Chem. Soc., Dalton Trans.*, 1991, 3413.
21 R. J. Abraham, G. H. Barnett, E. S. Bretschneider and K. M. Smith, *Tetrahedron*, 1973, **29**, 553.
22 R. J. Abraham, G. H. Barnett and K. M. Smith, *J. Chem. Soc., Perkin Trans. 1*, 1973, 2142.
23 K. M. Smith, *Chem. Commun.*, 1971, 540.
24 K. M. Kadish, B. Boisselier-Cocolios, A. Coutsolelos, P. Mitaine and R. Guilard, *Inorg. Chem.*, 1985, **24**, 4521.
25 J. P. Maher and D. F. Evans, *J. Chem. Soc.*, 1965, 637.
26 R. J. Abraham, G. E. Hawkes, M. F. Hudson and J. M. Smith, *J. Chem. Soc., Perkin Trans. 2*, 1975, 204.
27 J. E. Falk, *Porphyrins and Metalloporphyrins*, Elsevier, Amsterdam, 1976, p. 34.
28 K. M. Kadish, A. Tabard, A. Zrineh, M. Ferhat and R. Guilard, *Inorg. Chem.*, 1987, **26**, 2459.
29 K. M. Smith, *Org. Mass Spectrom.*, 1972, **6**, 1401.
30 (*a*) R. Faggiani and I. D. Brown, *Acta Crystallogr., Sect. B*, 1978, **34**, 2845; (*b*) K. Henrick, M. McPartlin, G. B. Deacon and R. J. Phillips, *J. Organomet. Chem.*, 1981, **204**, 287; (*c*) R. Faggiani and I. D. Brown, *Acta Crystallogr., Sect. B*, 1982, **38**, 2473; (*d*) Y. M. Chow and D. Britton, *Acta Crystallogr., Sect. B*, 1975, **31**, 1929; (*e*) H. Luth and M. R. Truter, *J. Chem. Soc. A*, 1970, 1287; L. Pauling, *Die Natur der Chemischen Bindung*, Verlag Chemie, Weinheim, 1968.
31 (*a*) M. S. Garcia-Tasende, B. E. Rivero, A. Castineiras, A. Sanchez, J. S. Cadas, J. Sordo, W. Hiller and J. Strähle, *Inorg. Chim. Acta*, 1991, **181**, 43; (*b*) G. H. W. Milburn and M. R. Truter, *J. Chem. Soc. A*, 1967, 648; (*c*) R. T. Griffin, K. Henrick, R. W. Matthews and M. McPartlin, *J. Chem. Soc., Dalton Trans.*, 1980, 1550.
32 D. M. Collins, R. Contryman and J. L. Hoard, *J. Am. Chem. Soc.*, 1972, **94**, 2066.
33 (*a*) H. Oumous, C. Lecomte, J. Protas, P. Cocolios and R. Guilard, *Polyhedron*, 1984, **3**, 651; (*b*) P. Cocolios, R. Guilard, D. Bayeul and C. Lecomte, *Inorg. Chem.*, 1985, **24**, 2058; (*c*) C. Lecomte, J. Protas, R. Guilard and P. Fournari, *J. Chem. Soc., Chem. Commun.*, 1976, 434; C. Lecomte, J. Protas, R. Guilard, B. Fliniaux and P. Fournari, *J. Chem. Soc., Dalton Trans.*, 1979, 1306; (*d*) J. L. Hoard, in *Porphyrins and Metalloporphyrins*, ed. K. M. Smith, Elsevier, Amsterdam, 1975, p. 317; (*e*) R. Guilard, C. Lecomte and K. M. Kadish, *Struct. Bonding* (*Berlin*), 1987, **64**, 205.
34 W. J. Baxter and G. Gafner, *Inorg. Chem.*, 1972, **11**, 176.
35 (*a*) Z. V. Zvonkova, *Zh. Fiz. Khim.*, 1956, **30**, 340; (*b*) J. Glaser, *Acta*

Chem. Scand., Ser. A, 1979, **33**, 789; (*c*) S. E. Jeffs, R. W. H. Small and I. J. Worrall, *Acta Crystallogr., Sect. C*, 1983, **39**, 1628.

36 (*a*) E. Gutierrez-Puebla, A. Vegas and S. Garcia-Blanca, *Acta Crystallogr., Sect. B*, 1980, **36**, 145; (*b*) H. Borgholte, K. Dehnicke, H. Goesmann and D. Fenske, *Z. Anorg. Allg. Chem.*, 1991, **600**, 7; (*c*) T. Watanabe, M. Atojii and C. Okazaki, *Acta Crystallogr.*, 1950, **3**, 405; (*d*) I. A. Kahwa, D. Miller, M. Mitchel, F. R. Fronczek, R. G. Goodrich, D. J. Williams, C. A. O'Mahoney, A. M. Z. Slawin, S. V. Ley and C. J. Groombridge, *Inorg. Chem.*, 1992, **31**, 3963; (*e*) G. Thiele, B. Grunvald, W. Rink and D. Breitinger, *Z. Naturforsch., Teil B*, 1979, **34**, 1520; J. Glaser, *Acta Chem. Scand., Ser. A*, 1980, **34**, 75.

37 K. Henrick, M. McPartlin, R. W. Matthews, G. B. Deacon and R. J. Phillips, *J. Organomet. Chem.*, 1980, **193**, 13; G. B. Deacon and R. J. Phillips, *J. Organomet. Chem.*, 1980, **199**, 15.

38 M. O. Senge, *J. Chem. Soc., Dalton Trans.*, in the press.

39 (*a*) M. R. Bermejo, A. Castineiras, J. A. Garcia-Vazquez, W. Hiller and J. Strähle, *J. Cryst. Mol. Struct.*, 1991, **21**, 93; (*b*) S. E. Jeffs, R. W. H. Small and I. J. Worall, *Acta Crystallogr., Sect. C*, 1984, **40**, 381; (*c*) I. A. Kahwa, D. Miller, M. Mitchel and F. R. Fronczek, *Acta Crystallogr., Sect. C*, 1993, **49**, 320; (*d*) W. Hiller, A. Castineiras, M. E. Garcia-Fernandez, M. R. Bermejo, J. Bravo and A. Sanchez, *Z. Naturforsch., Teil B*, 1988, **43**, 132; (*e*) S. E. Jeffs, R. W. H. Small and I. J. Worrall, *Acta Crystallogr., Sect. C*, 1984, **40**, 65.

40 C. Lecomte, J. Protas, J. C. Marchon and M. Nakajima, *Acta Crystallogr., Sect. B*, 1978, **34**, 2856.

41 M. R. Bermejo, A. Castineiras, M. Gayoso, W. Hiller, U. Englert and J. Strähle, *Z. Naturforsch., Teil B*, 1984, **39**, 1159.

42 K. F. Tebbe and U. Georgy, *Acta Crystallogr., Sect. C*, 1986, **42**, 1675.

43 (*a*) T. L. Blundell and H. M. Powell, *Proc. R. Soc. London, Ser. A*, 1972, **331**, 161; (*b*) G. B. Deacon, R. J. Phillips, K. Henrick and M. McPartlin, *Inorg. Chim. Acta*, 1979, **35**, L335; G. B. Deacon, S. J. Faulks, B. M. Gatehouse and A. J. Jozsa, *Inorg. Chim. Acta*, 1977, **21**, L1; (*d*) G. M. Sheldrick and W. S. Sheldrick, *J. Chem. Soc. A*, 1970, 28.

44 W. R. Scheidt, K. J. Haller and K. Hatano, *J. Am. Chem. Soc.*, 1980, **102**, 3017.

45 Y. M. Chow and D. Britton, *Acta Crystallogr., Sect. B*, 1975, **31**, 1922.

46 W. R. Scheidt, Y. J. Lee, D. K. Geiger, K. Taylor and K. Hatano, *J. Am. Chem. Soc.*, 1982, **104**, 3367; D. K. Geiger, V. Chunplang and W. R. Scheidt, *Inorg. Chem.*, 1985, **24**, 4736.

47 (*a*) B. C. Schardt, F. J. Hollander and C. L. Hill, *J. Am. Chem. Soc.*, 1982, **104**, 3964; (*b*) K. M. Adams, P. G. Rasmussen, W. R. Scheidt and K. Hatanao, *Inorg. Chem.*, 1979, **18**, 1892.

48 (*a*) M. Hörner, H. Fenner, J. Beck and W. Hiller, *Z. Anorg. Allg. Chem.*, 1989, **571**, 69; (*b*) R. Allmann, W. Henke, P. Krommer and J. Lorberth, *J. Organomet. Chem.*, 1978, **162**, 283.

49 C. Hebecker, *Z. Anorg. Allg. Chem.*, (*a*) 1972, **393**, 223; (*b*) 1975, **412**, 37.

50 D. M. Collins and J. L. Hoard, *J. Am. Chem. Soc.*, 1970, **92**, 3761.

51 M. P. Byrn, C. J. Curtis, I. Goldberg, Y. Hsiou, S. I. Khan, P. A. Sawin, S. K. Tendick and C. E. Strouse, *J. Am. Chem.*, 1991, **113**, 6549.

52 R. J. Abraham, F. Eivazi, H. Pearson and K. M. Smith, *J. Chem. Soc., Chem. Commun.*, 1976, 698, 699; M. O. Senge, K. R. Gerzevske, M. G. H. Vicente, T. P. Forsyth and K. M. Smith, *Angew. Chem., Int. Ed. Engl.*, 1993, **32**, 750; M. O. Senge, C. W. Eigenbrot, T. D. Brennan, J. Shusta, W. R. Scheidt and K. M. Smith, *Inorg. Chem.*, 1993, **32**, 3134.

53 H. Hope, *ACS Symp. Ser.*, 1987, **357**, 257.

54 H. Hope and M. Moezzi, XABS, University of California, 1987.

55 G. M. Sheldrick, SHELXTL-PLUS, Program for Crystal Structure Determination, Universität Göttingen, 1989.

Received 5*th May* 1993; *Paper* 3/02555A